2014•2015
FACULTEIT GENEESKUNDE EN LEVENSWETENSCHAPPEN
master in de biomedische wetenschappen

Masterproef

Consequences of spaceflight stressors on cell-mediated immunity

Promotor :
Prof. dr. Niels HELLINGS

Promotor :
dr. MARJAN MOREELS
Prof. dr. SARAH BAATOUT

Sebastiaan Deckers

Scriptie ingediend tot het behalen van de graad van master in de biomedische wetenschappen

2014•2015
FACULTEIT GENEESKUNDE EN LEVENSWETENSCHAPPEN
master in de biomedische wetenschappen

Masterproef

Consequences of spaceflight stressors on cell-mediated immunity

Promotor :
Prof. dr. Niels HELLINGS

Promotor :
dr. MARJAN MOREELS
Prof. dr. SARAH BAATOUT

Sebastiaan Deckers

Scriptie ingediend tot het behalen van de graad van master in de biomedische wetenschappen

universiteit hasselt | Maastricht University

Acknowledgements

This master thesis is the final conclusion of my five-year education of Biomedical Sciences at Hasselt University. Choosing an internship project was straightforward for me, as one topic at the Belgian Nuclear Research Centre (SCK•CEN) immediately stood out, "*Consequences of space flight stressors on adaptive immunity - Evaluation of immunological changes using space-simulated in vitro models".* I have always been fascinated by the space environment and the mysteries of the universe. The combination of space research and experimental lab work matched perfectly for me. Therefore, I greatly appreciate the given opportunity and would like to thank numerous people.

First, I would like to express my sincerest gratitude to my external promoters, Dr. Marjan Moreels and Prof. Dr. Sarah Baatout. They were the first to introduce me to the interesting field of radiobiology and kindly gave me the opportunity to complete my master thesis and perform real space research at SCK•CEN. I want to thank them for their support and for letting me attend numerous of exciting events such as an underground laboratory (HADES) visit, a two-week course on radiation protection, a European space project meeting and a live in-flight call with an ISS-crewmember. Furthermore, I want to thank my institutional supervisor, Prof. Dr. Niels Hellings for getting me acquainted with this internship topic and for his advice during progress meetings. My appreciation also goes to my second examiner, Prof. Dr. Veerle Somers for reading this report.

My special thanks go to my daily supervisor, PhD student Merel van Walleghem, who guided me throughout the laboratories, helped me with practical work and gave me much appreciated feedback on my thesis. Moreover, I would also want to thank Kevin Tabury and Ann Janssen for assisting me with Luminex technology.

Not to forget, my upmost gratitude goes to all the subjects who kindly donated blood in the name of science and to all the members of the Radiobiology Unit for creating such a pleasant working environment. Finally, I want to thank my family and friends for their support and belief in me, without them I would not have come this far.

Table of Contents

List of abbreviations

1 x g	Earth's gravity
µG	Microgravity
AP-1	Activator Protein 1
APC	Allophycocyanin
BD	Becton, Dickinson and Company
CD45	Leukocyte Common Antigen
CME	Coronal Mass Ejection
CMI	Cell-Mediated Immunity
CREB	cAMP Response Element-binding Protein
DB	Diluted Blood
DTH	Delayed-Type Hypersensitivity
EBV	Epstein-Barr Virus
ELISA	Enzyme-linked Immunosorbent Assay
ESA	European Space Agency
FACS	Fluorescent Activated Cell Sorting
FITC	Fluorescein isothiocyanate
FSC	Forward scatter
GCRs	Galactic Cosmic Rays
HC	Hydrocortisone
HPA	Hypothalamus-Pituitary-Adrenal
HZE	High-mass (Z), high-energy (E) particle
IR	Ionizing Radiation
IL-1	Interleukin-1
IL-1ra	Interleukin-1 receptor antagonist
IL-2	Interleukin-2
IL-2R	Interleukin-2 Receptor
IL-6	Interleukin-6
IL-10	Interleukin-10
IFN-γ	Interferon-gamma
ISS	International Space Station
LET	Linear-Energy Transfer
MNC	Mononuclear Cell
MoCISS	Monitoring Cellular Immunity on the International Space Station
NASA	National Aeronautics and Space Administration
NK	Natural Killer
NF-κB	Nuclear Factor kappa-light-chain-enhancer of activated B cells
PBMCs	Peripheral Blood Mononuclear Cells
PBS	Phoshate Buffered Saline
PI	Propidium Iodide
PIG	Pre-immunization Goat Serum
PKA	Protein Kinase A
PWM	Pokeweed Mitogen
RBC	Red Blood Cell
RPM	Random Positioning Machine
RPMI	Roswell Park Memorial Institute 1640 medium
s-µG	Simulated microgravity
SCK•CEN	Belgian Nuclear Research Centre
SPEs	Solar Particle Events
SSC	Side Scatter
STAT1	Signal Transducer and Activator of Transcription 1
STS	Space Transport System
TCR	T Cell Receptor
Th1	T helper type 1
Th2	T helper type 2
TNF-α	Tumor Necrosis Factor alpha
US	United States (of America)
WB	Whole Blood
WBC	White Blood Cell

Summary

INTRODUCTION: Astronauts in space encounter numerous spaceflight-associated factors causing both physical and psychological stress. Immune studies in space have shown that during space travel the immune system can be weakened. However, the adverse impact of specific factors and their underlying molecular mechanisms are not yet fully understood. In this project, we investigate the effect of simulated microgravity (s-µG) on cell-mediated immunity (CMI) and its potential modulation through stress hormones using the *in vitro* Delayed-Type Hypersensitivity (DTH) assay. Moreover, this work is set up to aid in the ground-based preparation of an immunology experiment in space, directed by the European Space Agency (ESA) in order to monitor the cellular immunity of astronauts during long-term space missions.

MATERIAL & METHODS: The *in vitro* DTH assay was performed under s-µG using the desktop Random Positioning Machine (RPM). Due to the random 3D movement during µG-simulation, closed tubes need to be used to prevent leakage. In a first step, the influence of s-µG and the use of closed cryotubes on the viability of the immune cells in whole blood samples was assessed. Two viability assays (Annexin V-FITC/PI and fluorescent amine-reactive labeling) were compared. Next, the individual and combined effects of s-µG and stress hormones on the CMI were assessed by performing the *in vitro* DTH assay under s-µG with the addition of hydrocortisone. During this assay, the immune cells in the samples were exposed to different immunogenic challenges (i.e. plant lectins, bacterial recall antigens, monoclonal anti-CD3/CD28 antibodies), thereby evoking an immune reaction. The CMI was evaluated by simultaneously measuring the concentration of four cytokines (IL-2, IFN-γ, TNF-α and IL-10) with Luminex technology.

RESULTS: Our results indicate that the viability of the immune cells is not greatly affected by s-µG and the use of closed cryotubes (i.e. no gas exchange) after 24 h of exposure to simulated spaceflight conditions. Multiplex cytokine analysis showed changed cytokine profiles after exposure to s-µG compared to donor-matched controls under Earth's gravity (*1 x g*). In addition, the evoked immune response varied for the different immunogenic challenges.

DISCUSSION & CONCLUSION: The *in vitro* DTH assay can be used to evaluate the effects of simulated space stressors on the immune response. Furthermore, the observed alterations in the cytokine profiles can give insight into the mechanisms whereby the space stressors affect the immune response. Moreover, the data obtained in this project may aid in identifying potential countermeasures for the detrimental effects of spaceflight, as well as help to understand other immune-suppressed conditions on Earth. In conclusion, space technology is rapidly advancing and strives to expand our current knowledge and boundaries of space exploration. This progression will inevitably lead to longer and more frequent stays in space. Therefore, the need to identify measures that can safeguard the health of astronauts during long-duration spaceflight, becomes an absolute priority.

Samenvatting (Dutch translation)

INLEIDING: Tijdens ruimtemissies komen astronauten voortdurend in contact met allerlei omgevingsfactoren die zowel op fysisch als psychisch vlak tot stress leiden. Immunologische studies in de ruimte hebben reeds aangetoond dat het immuunsysteem verzwakt kan worden. De precieze onderliggende moleculaire oorzaak daarvoor is echter nog niet volledig ontrafeld. In dit project wordt door middel van de *in vitro* vertraagd-type overgevoeligheidstest (Delayed-Type Hypersensitivity, DTH, test) het effect van gesimuleerde gewichtloosheid (s-µG), alsook het toevoegen van stress hormonen, op de celgemedieerde immuniteit (CMI) onderzocht. Dit werk maakt deel uit van de voorbereiding op een immunologisch ruimtevaart-experiment op het internationaal ruimtevaartstation (ISS), gegecoördineerd door het Europees Agentschap voor Ruimtevaart (ESA), met als doel het opvolgen van de CMI van astronauten gedurende lange ruimtevaart-missies.

MATERIAAL & METHODEN: De *in vitro* DTH test werd uitgevoerd in s-µG gebruikmakende van de desktop Random Positioning Machine (RPM). Doordat de samples tijdens de simulatie in drie dimensies bewegen, werden gesloten tubes gebruikt om lekkage te vermijden. In een eerste stap werd de invloed van s-µG en de gesloten tubes op de viabiliteit van de immuuncellen in humaan bloed nagegaan. Hiervoor werden twee viabiliteitstesten (Annexin V-FITC/PI and fluorescent amine-reactive labeling) gebruikt. Verder werden zowel de individuele invloeden, alsook het gecombineerde effect van s-µG en stress hormonen op de CMI onderzocht door de *in vitro* DTH assay tijdens µG-simulatie uit te voeren met toevoeging van hydrocortisone. Gedurende deze test werden de immuuncellen gestimuleerd met verschillende immunogene stimuli (challenges), zoals plantlectines, bacteriële recall antigenen en monoclonale anti-CD3/CD28 antilichamen. De uitgelokte immuunrespons werd ten slotte geëvalueerd door simultaan vier cytokine concentraties (IL-2, IFN-γ, TNF-α and IL-10) te meten via Luminex technologie.

RESULTATEN: De bekomen resultaten tonen aan dat de immuuncel-viabiliteit niet merkbaar beïnvloed wordt door 24 uur s-µG en het gebruik van gesloten tubes (geen gasuitwisseling). De meervoudige cytokine analyse onthulde gewijzigde cytokine profielen onder s-µG, in vergelijking met de controle stalen van identieke donoren onder normale zwaartekracht (*1 x g*). De immuunrespons was eveneens variabel na stimulatie met verschillende immunogene stimuli.

DISCUSSIE & CONCLUSIE: Met de *in vitro* DTH test kunnen de effecten van s-µG en stress hormonen op de immuunrespons opgevolgd worden. De gemeten verschillen in cytokine profielen geven aanwijzingen naar de onderliggende moleculaire werkingsmechanismen waarmee de onderzocht ruimte-factoren de immuunrespons beïnvloeden. De verkregen resultaten kunnen eveneens helpen in het identificeren van potentiële middelen die de schadelijke effecten van ruimtevaart kunnen tegenwerken, alsook in het beter begrijpen van andere immunosupressieve aandoeningen op aarde. Ten slotte wordt de ruimtevaarttechnologie steeds verder geoptimaliseerd en de limieten van de ruimtevaart exploratie worden voortdurend verlegd. Die progressie zal onvermijdelijk leiden tot zowel langere als meer talrijke ruimtemissies. Hierdoor is de nood naar het identificeren van middelen die de gezondheid van astronauten in stand kunnen houden gedurende langdurige ruimtemissies een absolute prioriteit.

I. Introduction

1. Human space exploration

The human intuitive nature to explore and search for new scientific or social clues in life, has guided mankind into developing a new era of space exploration beyond the scope of Earth. In April 1961, a Soviet cosmonaut named Yuri Gagarin, became the first human to orbit the globe in a single-manned satellite. His historical journey lasted 108 minutes and was the first major milestone in human space exploration. Since then, space technology is rapidly enhancing, driven by prestige and rivalry between international space organizations. The United States (US) lined up the Apollo program for manned space missions in 1968, directed by the National Aeronautics and Space Administration (NASA). On the 20th of July, 1969, the long anticipated first lunar landing was no longer fiction, as for the lunar module of Apollo 11 had landed on the Moon's surface. Crew members Neil Armstrong and Edwin Aldrin became the first humans to ever set foot on a celestial body other than planet Earth. Even though great triumphs had already been accomplished, the deep desire to further explore the universe gained interest. This lead to the development of the space shuttle (i.e. Space Transport System, STS), which was the first partially reusable space craft that could perform multiple low Earth orbital space operations. Once again, the field of space technology leaped forward greatly and the idea of constructing a permanent orbital space station such as the International Space Station (ISS) was born. Sustaining astronauts in space for extended periods of time (i.e. multiple months) became feasible, and accordingly, the prospect of long-duration space missions commenced.

In future space missions we continuously strive to reach out further into the unexplored areas of our universe. Human settlement on Mars is currently the next enormous project, regarding the immense distance that has to be covered and the amount of time needed to be spent in space (i.e. 520-day Mars mission). In addition to the technical challenges, extended duration space travel also entails some medical risks concerning human health in space. The human body must endure a multitude of environmental changes during space travel such as decreased gravitational force (i.e. perceived as weightlessness), exposure to harmful cosmic radiation and psychological pressure due to confinement, sleep deprivation and heavy workload. Accordingly, long-duration spaceflight is accompanied with the dysregulation of the human physiology, which includes our research topic regarding a reduced immune response efficiency (1). Therefore, scientific attention is needed in order to establish the necessary countermeasures that ought to prevent or mitigate the medical risks of future space missions.

2. The space environment: impact on the human physiology

On Earth, any person's disease can be generally characterized as an abnormal human physiology in a normal environment. In contrast, astronauts who undergo extensive medical screening to ensure a healthy physiology, will face an abnormal environment (i.e. space) after mission launch. During spaceflight, astronauts are subjected to different environmental factors (i.e. stressors), which are related to the attenuation of human health and will be referred to as "space stressors".

Since all life has evolved under the influence of Earth's gravity (*1 x g*), it is acceptable to assume that the microgravity (µG) environment in space will have a substantial physiological impact on space travelers. Moreover, exposure to harmful cosmic radiation is inevitably linked with space exploration and could contribute to additional dysregulation of the normal physiology. In addition, astronauts are prone to experience psychological stress in space, which might modulate various physiological processes as well. Thus, in order to fully comprehend the disadvantageous consequences of the spaceflight, additional space research is necessary.

2.1. Physical space stressors of the cosmos

The most fundamental physical space stressors are inherently present throughout space and consist of µG and radiation (2).

2.1.1. The microgravity environment of space

One major and well known factor of the space environment is µG. This factor is often wrongfully confused with weightlessness, but µG actually explains a situation in which the gravitational force working on an object, seems to be very small (i.e. "micro"), but is not absolute zero. For instance, the ISS orbits Earth at the height of approximately 400 km above ground. At this altitude, Earth's gravitational force has merely undergone a 10% decrease compared to sea level, e.g. an 80 kg-astronaut on Earth would still weigh 72 kg on the ISS. However, the fast-moving ISS is actually continuously falling towards Earth (i.e. free fall), making the crew members inside the space station, all travelling at that same orbital speed, seemingly weightless to the environment. Long-duration spaceflight research on board space stations, such as the ISS, has aided immensely in describing the detrimental consequences of the space environment on the human physiology.

Biological effects of microgravity

As mentioned before, the basic architecture of all biological systems on Earth evolved under gravity. The µG-related effects on astronauts in space lead to considerable complications on a variety of organ systems. Described human health changes as a consequence of µG include body fluid distribution (i.e. from lower extremities to the head), loss of bone and muscle mass, disturbed neurovestibular and proprioceptive system (i.e. space motion sickness) (3), and attenuation of the immune response (4). At first sight, the harmful implications of µG on the astronauts' health in space, oppose significant threat to further space exploration. However, it has become apparent as well that such human organic systems show great adaptation capabilities to stress (i.e. µG), and usually after several weeks the main adverse effects are compensated, except for loss of bone and muscle mass. Consequently, the limiting factor of extended duration space missions will, most likely, not be µG, but instead the prolonged exposure to harmful cosmic radiation and psychological stress (5).

2.1.2. The space radiation environment

Cosmic radiation is, similar to µG, inherently existent throughout the entire universe. In fact, cosmic rays are particles (i.e. atomic nuclei or electrons) which are travelling at high-speed through space.

Such particles can either originate from the Sun during solar flares or coronal mass ejections (CMEs), known as solar particle events (SPEs), or come from other sources within the Milky Way Galaxy (i.e. exploding stars), defined as galactic cosmic rays (GCRs) (Fig. 1). High-energy primary GCRs that arrive at the outer edge of Earth's atmosphere will collide with other atmospherical nuclei to form short-lived secondary cosmic rays (e.g. neutrons). Primary cosmic rays exist of 2% electrons and 98% atomic nuclei, of which 86% protons, 11% alpha particles and < 1% high-mass (Z), and high-energy (E), (HZE) particles (e.g. iron). However, specifically, this latter fraction is very important because of its high linear-energy transfer (LET, i.e. measure for energy transfer from an ionizing particle passing through matter). The LET-value of a radiation particle relates to the observed biological effects on astronauts. Furthermore, space operation characteristics such as trajectory, mission duration and space craft model, are all involved in the relative exposure to radiation of astronauts (5).

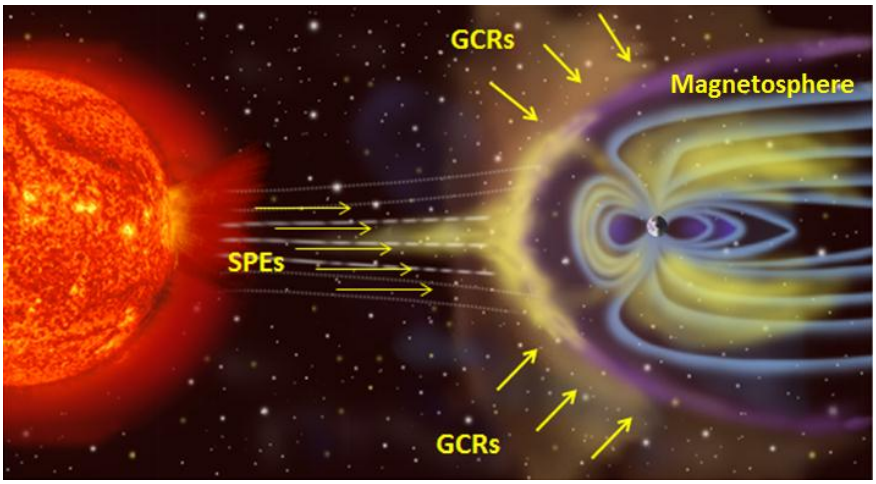

Figure 1. Types of radiation in space (6).

On Earth, humans are primarily exposed to background radiation through the inhalation of air, ingestion of food, penetrating cosmic radiation and through terrestrial radiation from the soil (e.g. radon) (6). The human radiation dose, expressed in Sieverts (Sv, dose equivalent radiation) is approximately 2-3 µSv/day at the Earth's surface, but increases to 200-600 µSv/day during low Earth orbital missions (e.g. on the ISS) and even more during interplanetary space exploration (5). This increase in radiation exposure is related to the Earth's magnetosphere, which attenuates (i.e. "traps") incoming cosmic rays close to Earth (Fig. 1). Additionally, HZE particles (i.e. from deep space) can not be stopped by current space craft shielding materials. Accordingly, radiation dose in space is much higher compared to Earth.

Indeed, recent data obtained from the Curiosity ranger (i.e. shielded inside a spacecraft) on its 253-day trip to Mars, indicated an average GCR dose equivalent rate of 1.84 mSv/day (7). Furthermore, the average dose equivalent rate of radiation on Mars' surface is found to be 0.64 ± 0.12 mSv/day. Using modern technology, the total cumulative mission dose for the shortest possible round-trip to Mars, with a 500-day stay on the planet, is estimated to be ± 1.01 Sv (8). Since the Russian, European and Canadian space agencies apply a 1 Sv exposure limit for the complete career of astronauts, this implies that they could exceed their career limit in one trip (7).

Biological effects of radiation

The biological consequences of ionizing radiation (IR) on human physiology are diverse, ranging from acute radiation sickness (i.e. nausea, weakness, skin burns or organ failure) caused by exposure to high dose rates of radiation, to long-term effects such as cataract development (9) and an increased carcinogenic risk via chronic damage of DNA molecules (10) and other macromolecules (i.e. lipid peroxidation). The living tissue is injured through a process called ionization, in which IR induces DNA damage in living cells directly, or indirectly through the radiolysis of water (11). In particular, rapidly proliferating cells such as hematopoietic cells are especially radiosensitive to IR (5).

2.2. Psychological stress related to spaceflight

It is well-documented that prolonged exposure to physical space stressors (i.e. µG and radiation) dysregulates the human physiology of astronauts during long-term space missions. However, the astronaut's mental well-being is also affected in space by a variety of psychological, interpersonal and psychiatric parameters related to long-duration spaceflight (12). The general health of the astronaut depends on the individual capability to cope with changes caused by physical stress, as well as psychological stress (13) induced by long-term isolation, sleep-deprivation, high work-load, loss of privacy and monotonous confinement (14). Consequently, difficulties in coping with such types of psychological stress might lead to diminished cognitive performance of astronauts and could therefore potentially interfere with the accomplishment of key mission goals. Additionally, interpersonal tension and numb group dynamics due to the social monotony (i.e. small crew size) and forced social interaction are potential risk factors during long-term space missions. Therefore, group member cohesion and encouragement to engage reasoning are very important social aspects in order to withstand long-duration space travel in the future.

3. Dysregulation of the immune system in space

The immune system is composed of various cell types with distinct morphology and functions. These cells either reside in structured peripheral tissues (e.g. spleen, thymus, lymph nodes, and tonsils) or recirculate in the body via the cardiovascular and lymphatic systems. The immune system offers targeted protection against different types of pathogenic microbes such as bacteria, viruses, parasites or fungi, by means of specifically recognizing microbial patterns that guide the immune response. However, since the Apollo and Skylab missions in the 1970s it became evident that spaceflight dysregulated the immune system of astronauts in space. Numerous crew members suffered from in-flight infections and showed diminished immune function post-flight (15). Consequently, sustaining human health in space could be hindered by long-duration stays in space.

3.1. Diminution of the immune response during spaceflight

Fifty years of space research has revealed many potential hazards regarding human health and immunity during spaceflight (4), however the accurate clinical significance of such harmful effects still remains unidentified. Thus, in order to advance towards extended duration space voyages (i.e. interplanetary space travel), the immunosuppressive effects of spaceflight need to be considered even more thoroughly.

3.1.1. Attenuated immune competence under microgravity

Multiple components of the immune system are altered under µG. The immune system can be divided into two interconnected systems consisting of the innate immunity (i.e. "first line of defense") and the adaptive immunity (i.e. "second line of defense"). Firstly, the nonspecific innate immune response is intrinsically present and is mediated by the complement system, phagocytes (e.g. neutrophils, macrophages, dendritic cells) and natural killer (NK) cells. Secondly, the adaptive immune response is a delayed, antigen-specific reaction which is mediated by B and T lymphocytes and has the capacity to retain immunological memory (i.e. long-lived memory lymphocytes) after resolution of the infection.

Peripheral leukocyte populations

To date, numerous independent studies (reviewed by Guéguinou et al.) have reported alterations in leukocyte (i.e. white blood cell, WBC) populations of experimental animals and humans during or following spaceflight (4). Analyzing peripheral leukocyte distributions in different clinical situations is frequently used to investigate *in vivo* immune function. Even though a high variability exists between studies, the most consistent findings indicate an increase in neutrophils and a decrease in lymphocytes and monocytes due to spaceflight conditions. More specifically, among the lymphocyte subsets, T and NK cell percentages are regularly decreased, but changes in B cell percentages are various. Crucian et al. compared human leukocyte populations during short-term (i.e. 12-14 days) versus long-term (i.e. 179-515 days) spaceflight. They reported a reduction in total peripheral blood lymphocyte number, a decrease in NK and senescent T cell percentages, but an increase in neutrophil, memory T and B cell percentages at landing, compared to preflight values (16).

Functional changes in peripheral leukocytes

Spaceflight does not only affect the number and distribution of peripheral leukocytes, but it also influences important cellular processes such as phagocytosis, microbial killing (i.e. oxidative burst), as well as lymphocyte activation, proliferation and cytokine production. The phagocytic properties (e.g. microbe engulfing and killing) of neutrophils (17) and monocytes (18) were diminished after spaceflight. Additionally, in a study of Rykova et al. on 30 cosmonauts who flew on the ISS during both short- and long-term space missions, they found that NK cell cytotoxicity was suppressed compared to pre-flight data (19). Moreover, proliferative responses of naïve T cells to mitogens (i.e. induction of T cell activation and clonal expansion) were lower at landing in multiple subjects after long stays in space.

Blunting of T cell activation

Normally, full T-cell activation (Fig. 2) requires antigenic peptide presentation on the T cell receptor (TCR), binding of interleukin-2 (IL-2) cytokine and co-stimulation via interleukin-1 (IL-1) or B7 protein interaction delivered by accessory cells (e.g. antigen presenting cells, monocytes). The first signal (Fig. 2A), which is TCR/antigen interaction was not affected *in vitro* by µG conditions in human peripheral blood and Jurkat T cell lines. However, the secretion and expression of IL-2, as well as IL-2 Receptor (IL-2R) surface expression (Fig. 2B) on T cells are strongly repressed during spaceflight (20, 21).

Consequently, the IL-2 signaling inhibition in T cells during spaceflight, significantly hindered important downstream effects such as early T cell activation, proliferation and differentiation into effector T cells. Co-stimulatory signaling (Fig. 2C) might also be hampered in space through a mismatch in cellular motility between on the one hand highly motile T cells, and on the other hand relatively immobile accessory monocytes (4).

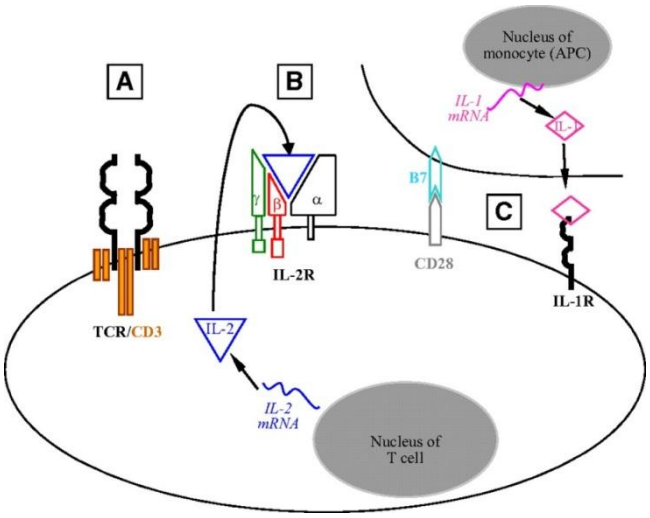

Figure 2. Required signals for T cell activation (4).

Cytokine profile dysregulation

Many studies have reported alterations in human cytokine profiles of lymphocytes during spaceflight (i.e. in-flight) or directly upon landing. Secretion of IL-2 and interferon gamma (IFN-γ) was decreased post-flight for both short and long-term space missions (16). In-flight cytokine data showed elevated production of tumor necrosis factor alpha (TNF-α), but reduced production for IFN-γ and interleukin-10 (IL-10) (22). Additionally, the secreted IFN-γ/IL-10 ratio was reduced independent from space mission duration. Since IFN-γ is known to inhibit the development of a T helper type 2 (Th2) cytokine profile, these findings suggest that μG might induce a shift to a Th2 immune response (4).

Changes in gene expression

Impaired T cell function due to altered gravity could also be caused by changes in gene expression. Indeed, Boonyaratanakornkit et al. measured differentially expressed genes regarding T cell activation in human T cells under modeled μG. Moreover, they found that the majority of early T cell activation genes were regulated by the transcription factors nuclear factor kappa-light-chain-enhancer of activated B cells (NF-κB), cAMP response element-binding protein (CREB), Ets-like protein, activator protein 1 (AP-1) and signal transducer and activator of transcription 1 (STAT1). Thus, these transcription factors seem to be key players in μG-mediated gene expression alteration. Accordingly, this implies that a multitude of downstream target genes involved in proliferation, apoptosis, biosynthesis or secretion will be affected by spaceflight (21).

Microbial resilience and latent virus reactivation

Spaceflight dysregulates various immunoregulatory processes, that could in turn interfere in the astronaut's ability to protect himself from infections and disease. In addition to immune system dysregulation, many studies reported alterations in the characteristics of pathogens. Accordingly, bacteria demonstrated superior features in space conditions such as enhanced virulence, exponential growth and thickening of the microbial wall (23). In addition, it has been shown that in-flight exchange of microbial intestinal flora and cross-contamination of opportunistic pathogens such as S. Aureus is possible between crew members (24). Finally, the reactivation of latent viruses (e.g. herpes virus) in astronauts during spaceflight is described as well (25).

3.1.2. Impact of radiation on immune system function

Similar to µG, radiation is always present in space and is known to influence the immune system. Most studies about radiation consist of reproducable Earth-based animal (i.e. rodents) experiments. Such ground-based studies indicate that both acute, as well as chronic exposure to IR, cause alterations in immune function. Radiation dose is measured in gray (Gy) and the impact on the human body depends on the dose rate (i.e. radiation dose per time unit) and the subsequent radiobiological effects.

Acute exposure to high doses of radiation in space

In the context of astronauts in space, acute radiobiological effects result from exposure to high-dose radiation (i.e. > 1 Gy) such as SPEs over a short period of time (e.g. hours, days). Many studies investigated the effect of a single exposure to a high dose (e.g. 3 Gy) of radiation on the immune system. For instance, Pecaut et al. studied the impact of low-LET γ-radiation on both lymphocytes as well as lympoid organs (i.e. spleen) in mice. Four days after a single exposure up to 3 Gy, they found a dose-related decrease in blood leukocyte number and spleen mass. Morever, there were variations in radiosensitivity among different lymphocyte subsets in both spleen and blood. In detail, B cell subsets markedly deceased (i.e. high radiosensitivity), whereas NK cell proportions remained relatively stable (i.e. low radiosensitivity). Within the T cell subset, $CD4^+$ T helper cells were more radiosensitive compared to $CD8^+$ cytotoxic T cells (26). Furthermore, in a parallel study they compared proton with γ-irradiation (i.e. same dose of 3 Gy) and found a more profound dysregulation of the immune system after proton irradiation (27). In addition, single high-LET irradiation (e.g. iron ions, up to 3 Gy) also caused analogous dose-dependent decreases in lymphoid organ mass and leukocyte population number (28).

Chronic exposure to low doses of radiation during spaceflight

Zeitlin et al. reported an average radiation dose of 0.481 ± 0.08 µGy/day for a 253-day trip to Mars (7). Accordingly, the continuous (i.e. chronic) exposure to low dose or low-dose-rate (LDR) radiation is closely related to long stays in space. Moreover, the daily radiation dose of an astronaut in space depends on either the protracted exposure to LDR radiation, as well as possible acute exposure during SPEs.

Rizvi et al. investigated this potentially perilous situation by exposing mice to LDR γ-radiation (i.e. total 0.01 Gy, 0.179mGy/h), directly succeeded with an additional exposure to simulated high-dose SPEs (i.e. 1.7 Gy simulated SPE protons). They indicated that prolonged LDR γ-irradiation can modify the subsequent effects of simulated SPE protons on the immunomodulatory response of $CD4^+$ T helper cells (29).

3.2. Modulation of the immune response through psychological stress

Psychological stress is controlled by the brain via the activation of the hypothalamus-pituitary-adrenal (HPA) axis and nervous system. The stress response is mediated by a multitude of secreted biomolecules such as the adrenal stress hormones (e.g. cortisol and adrenaline) as well as pro- and anti-inflammatory cytokines. All these mediators are linked together into a highly regulated, interactive network which can affect the stress response in many ways (30).

Psychosocial effects of long-term isolation and confinement

The effects of psychological stress during long-duration spaceflight have primarily been studied on Earth using isolation and confinement experiments. For instance, the Mars-500 project (Fig. 3) simulated a 520-day mission to Mars aiming at unravelling the impact of prolonged psychological stress (i.e. isolation, confinement) on the human physiology. Results of this study have shown that long-term isolation leads to elevated stress hormones levels (i.e. cortisol), increased lymphocyte number and intensified immune responses against common viral infections. This data suggests that chronic psychological stress can indeed trigger alterations in leukocyte phenotype, as well as yield dysregulated immune responses (31).

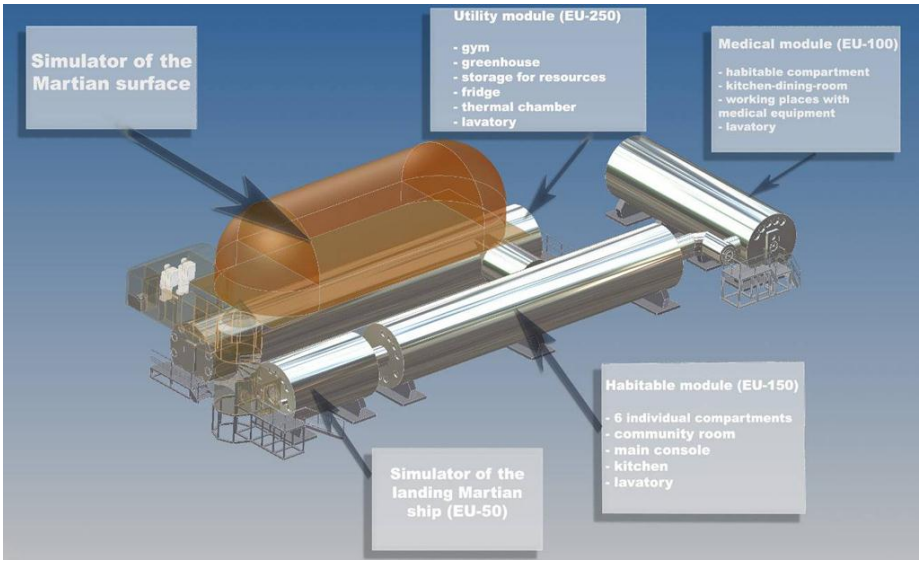

Figure 3. The Earth-based Mars-500 facility mimicking a 520-day mission to Mars. (Source: ESA)

Furthermore, multiple immune parameters were analyzed during a confinement study on Antarctica (i.e. Australian Antarctic Reasearch Centre), in which subjects were isolated for 9 months. In this study, Tingate et al. found that immune function was altered through changes in cytokine production such as TNF-α, IL-1, IL-2, IL-6, IL-1ra and IL-10 (32). Moreover, long-term isolation on Antarctica was also associated with increased viral shedding (i.e. herpes virus) and an expansion of latent Epstein-Barr virus (EBV)-infected B cell populations.

4. Context thesis: an immunology experiment in space

My thesis aims at contributing towards the ground-based preparation of the European Space Agency (ESA) approved spaceflight project, "Monitoring Cellular Immunity on the International Space Station (MoCISS)". During this 6-month space mission, which will fly in 2016, the crew will perform in-flight immunological experiments using the *in vitro* Delayed-Type Hypersensitivity (DTH) assay. With this assay, the overall immune response of the astronauts can be evaluated, thereby demonstrating the underlying antigen-dependent memory and effector cell reactions (33). In my project, we want to evaluate the effects of simulated spaceflight conditions on the CMI response, and possible modulation of this response through stress hormones (i.e. hydrocortisone). Accordingly, we selected the *in vitro* DTH assay since it has the capacity to assess the global immune response and, even more importantly, it is approved for an in-flight experiment (MoCISS).

Hypothesis and research objectives

Astronauts in space encounter several space-associated factors which are known to cause both physical and psychological stress. Important findings indicate that the immune system can be dysregulated during spaceflight. However, the individual as well as the combined impact of specific stressors such as µG, IR and psychological stress on the immune system is not yet fully understood. The hypothesis of my project is that the different simulated spaceflight stressors have a combined and detrimental effect on the human cellular immune response.

In the first objective we optimize a cell viability assessment technique and aim at investigating leukocyte viability after incubating human blood samples for 24 h under s-µG in closed tubes (i.e. needed for the *in vitro* simulation of µG). Secondly, the immune cells in the blood samples are exposed to simulated spaceflight stressors and stimulated with different challenges to trigger lymphocyte activation and cytokine release using the *in vitro* DTH assay. After stimulation the alterations in cytokine concentrations are analyzed because of their competence to reflect changes in the efficiency of the immune system.

Relevance

Interplanetary travel (e.g. to Mars) will vastly increase the duration of future space missions. These plans are leading to the pressing need to identify candidates which can prevent the disadvantageous consequences of space travel. The outcome of this project contributes to generating new insights into the underlying mechanisms that are associated with the weakening of the immune system in space. These insights can aid in the identification of potential therapeutic measures, which can counteract the patho-physiological consequences of spaceflight-associated conditions on the human immune system. The provided academic knowledge will support sustaining the general health of astronauts in space, as well as contribute to a better understanding of other types of immune suppressed conditions that are present on Earth.

II. Materials and methods

1. Spaceflight analogues: simulating space conditions on Earth.

In this project Earth-based space research is performed at the Belgian Nuclear Research Centre (SCK•CEN). The first requirement was to simulate different spaceflight conditions on ground within the facility.

1.1. Ground-based simulation of microgravity

The µG environment of space was simulated with a desktop Random Positioning Machine (RPM; Dutch Space, Leiden, The Netherlands). The RPM (i.e. specialized two-axis clinostat) consists of a sturdy base-frame with two independently motorized rotating frames (i.e. outer and inner frame) (Fig. 4A). The RPM is connected to computer algorithms which coordinate continuous random changes relative to the gravity vector (i.e. 3D gravity-vector averaging; visualized in Suppl. Fig. 1A). In our experiments the real random motion mode was used, with a minimal and maximal frame rotation speed of 55°/s and 72°/s, respectively. Furthermore, both the direction of rotation as well as individual frame speed were set on random (i.e. random walk, Suppl. Fig 1B). Finally, temperature during culturing was regulated by placing the RPM inside an incubator at 37°C (Fig. 4B).

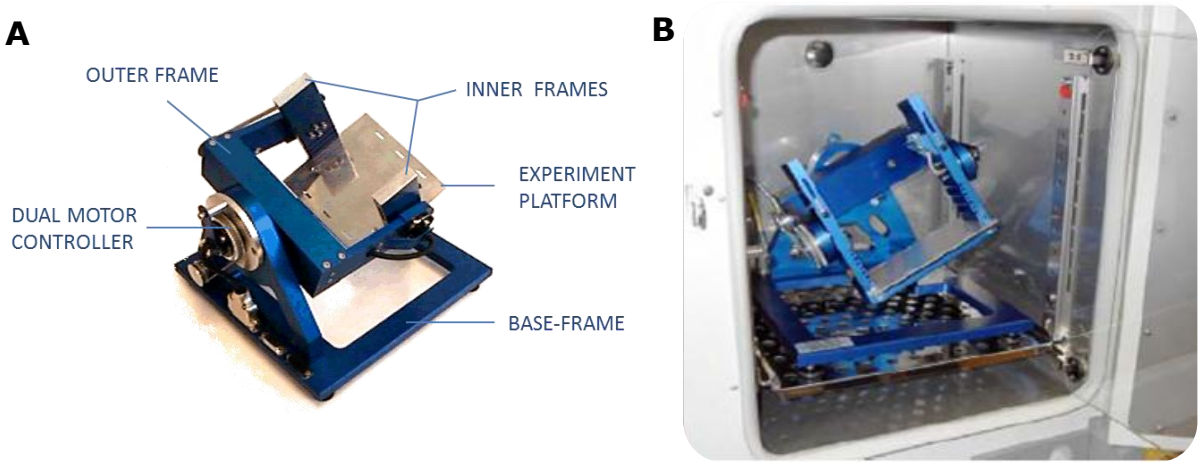

Figure 4. (A) The desktop Random Positioning Machine (RPM). **(B)** Desktop RPM in standard incubator (34).

1.2. Simulation of spaceflight-associated psychological stress

Psychological stress accompanied with long-duration spaceflight has been associated with increased levels of stress hormones in the blood. Based on these findings, the psychological stress response was simulated *in vitro* by the addition of hydrocortisone (HC) to the blood samples (0-100-200-400-600 ng/ml). Stress hormone-induced modulation of the cell-mediated immune response was analyzed using the *in vitro* DTH assay. In addition, the combined effect of simulated psychological stress (i.e. hydrocortisone), and s-µG (i.e. RPM), was investigated as well.

2. Collection and preparation of blood samples

Blood donation

After informed consent was given, peripheral blood was drawn from adult healthy volunteers in the morning (10-11 a.m.) into standard heparinized tubes by means of venipuncture. In general, blood from a single donor was used to analyze multiple test conditions. In order to prevent blood sedimentation and ensure thorough mixing, the filled blood tubes were stored on a rocking platform at room temperature to be processed within 2 h of drawing.

Blood preparation and incubation

Under aseptic conditions, peripheral whole blood (WB) was diluted in Roswell Park Memorial Institute 1640 medium (RPMI; Sigma-Aldrich Chemie GmbH, Steinheim, Germany), and subsequently transferred into round-bottomed 1.0 ml cryotubes (Thermo Fisher Scientific NUNC A/S, Roskilde, Denmark). Completely filled cryotubes (total assay volume 1500 µl) containing the diluted blood ($DB_{1:2}$, 50% v/v WB in RPMI) were closed (i.e. no gas exchange) and taped onto the RPM experiment platform for µG-simulation, or base frame (*1 x g* control) to start incubation. This way, all tubes are equally exposed to potential mechanical vibrations produced by the RPM.

3. Leukocyte isolation from peripheral blood

In vitro analysis of leukocytes is frequently hindered by the relatively high concentration of red blood cells (RBCs) in peripheral whole blood samples. Therefore, two different leukocyte purification procedures were examined separately in this project, i.e. selective red blood cell lysis and peripheral blood mononuclear cell (PBMC) isolation

Red blood cell lysis

Leukocytes in peripheral blood were isolated through hypotonic RBC lysis using either Fluorescent Activated Cell Sorting (FACS) lysing solution (BD, Becton Dickinson and Company, San Jose, CA, USA), or Promega Cell Lysis Solution (Promega Corporation, Madison, WI, USA). Detailed RBC lysis protocols are listed in the supplement (Suppl. Procedures I).

Peripheral blood mononuclear cell isolation

Aliquots of 3 ml $DB_{1:4}$ (25% v/v WB in RPMI) were added to pre-filled 15 ml-centrifuge tubes containing 3 ml density gradient medium (Histopaque; Sigma-Aldrich, St. Louis, MO, USA), and were centrifuged (400 *x g,* 30 min) to induce blood cell separation. Subsequently, the mononuclear cell layer (MNC; i.e. "buffy coat") containing PBMCs was transferred into new tubes and washed twice in Phosphate Buffered Saline (PBS; Life Technologies, Gibco, Grand island, NY, USA). Finally, after centrifugation (250 *x g*, 10 min), PBMCs were resuspended in 200 µl RPMI.

4. Viability labeling of isolated leukocytes

4.1. Detection of apoptotic CD45$^+$ leukocytes using the Annexin V/PI assay

Leukocyte viability was examined following blood collection (i.e. pre-incubation), or after 24 h of incubation at 37°C in normal gravity or under µG-simulation. Monoclonal antibodies against CD45 (i.e. common leukocyte antigen) were used to identify the leukocyte (i.e. CD45$^+$) subset. Furthermore, Annexin V-labeling of phosphatidylserine (PS) was used as a marker for early apoptosis and supplemental labeling with propidium iodide (PI) enabled distinction of viable from dead cells.

Annexin V/PI labeling after red blood cell lysis

Aliquots of 100 µl WB or 200 µl $DB_{1:2}$ were labeled with 5 µl monoclonal anti-CD45-APC antibodies (BD) and samples were incubated for 15 min in the dark at room temperature. Next, leukocytes were purified through hypotonic red blood cell (RBC) lysis using either FACS or Promega lysing procedures (Suppl. Procedures I). Afterwards, purified leukocytes were washed in PBS and labeled for PS (Annexin V-FITC) and nucleic acids (PI), according to the manufacturer's instructions (Annexin V-FITC Apoptosis detection kit, Affymetrix, eBioscience, Bender MedSystems GmbH, Vienna, Austria).

Annexin V/PI labeling after mononuclear cell isolation

PBMCs were isolated from aliquots of 3ml $DB_{1:4}$ and resuspended in 200 µl RPMI. Subsequently, the cell suspension was labeled with 5 µl anti-CD45-APC antibodies (BD) for 15 min in the dark at room temperature, washed in PBS and finally labeled with Annexin V-FITC and PI according to the manufacturer's instructions.

4.2. Detection of cell death using the near infrared LIVE/DEAD assay

Following blood collection, or after 24 h of incubation at 37°C with or without µG-simulation, the viability of the isolated PBMCs was measured using the LIVE/DEAD® Fixable near-IR Dead Cell Stain Kit (Life Technologies, Molecular Probes, Eugene, OR, USA). In short, PBMCs were resuspended in 1 ml PBS after isolation and subsequently labeled for 30 min with 1 µl of reconstituted, near-infrared fluorescent reactive dye on ice and in the dark. Subsequently, after washing once in PBS, 10 µl of monoclonal anti-CD3-FITC antibodies (BD) were added to 100 µl of cell suspension in PBS, and incubated for 15 min at room temperature. Excess of antibodies were washed away and PBMCs were fixed in 1 ml of 3.7% formaldehyde (Sigma-Aldrich Chemie GmbH, Steinheim, Germany) in PBS for 15 min at room temperature. Afterwards, fixed PBMCs were washed once with 1% pre-immunization goat serum (PIG) in PBS and resuspended in 500 µl 1% PIG in PBS and stored on ice until flow cytometric analysis.

5. Flow cytometric analysis of cell viability

Data of the viability labeling was collected with the Accuri C6 Flow Cytometer (BD, Fig. 5) and analyzed using the manufacturer's BD Accuri™ C6 Software (v. 1.0.264.21). For data acquisition, the forward scatter (FSC) threshold was set on 300.000 to minimize the collection of small-sized background events (i.e. platelets, cellular debris), without losing sensitivity for leukocyte detection.

Figure 5. The Accuri™ C6 Flow Cytometer and standard viability plot.

Measuring Annexin V/PI labeling of CD45⁺ leukocytes

Green (FL1-detector), and orange-red (FL3-detector) fluorescence signals from Annexin V-FITC and PI, respectively, were collected after exposure to a blue 488 nm solid state laser, whereas red (FL4-detector) fluorescence signals from anti-CD45-APC was collected after exposure to a red 640 nm diodode laser (Table 1). The leukocyte population (i.e. $CD45^+$ subset) was gated, based on a dot-plot displaying the side scatter (SSC) and FL4 (APC) properties of the collected events after flow cytometric analysis. Subsequently, viability of the cells was analyzed via FL1 vs. FL3 dot-plots (i.e. Annexin V-FITC vs. PI) (Fig. 5) displaying marked regions of viable cells (i.e. Annexin V^-/PI^- gate), early apoptotic cells (i.e. Annexin V^+/PI^- gate) and dead cells (i.e. Annexin $V^{(-/+)}/PI^+$ gate).

Table 1. Flow cytometer settings Annexin V/PI analysis

Detector	Laser	Emission filter (nm/BP)	Fluorophore	Antibody conjugation
FL1	488 nm	533/30	FITC (green)	Annexin V
FL2	488 nm	585/40	-	-
FL3	488 nm	670/LP	PI (orange-red)	-
FL4	640 nm	675/25	APC (red)	Anti-CD45

BP: Band Pass width. LP: Long Pass. FITC: Fluorescein isothiocyanate. PI: Propidium Iodide. APC: Allophycocyanin.

Measuring near-infrared labeling of cellular amines in peripheral blood mononuclear cells

Green fluorescent emission light from anti-CD3-FITC, was collected (FL1-detector) after excitation with a blue 488 nm solid state laser, whereas the near-infrared fluorescent emission light from the near-infrared fluorescent reactive dye was collected (FL4-detector) after exposure to a red 640 nm diodode laser (Table 2). The T lymphocyte subset (i.e. $CD3^+$ subset) was identified based on dot-plots displaying SSC and FL1 (FITC) properties of the collected events. Subsequently, viable cells were discriminated from unviable cells based on, respectively low and high FL4 (near-infrared) signals, displayed in count plots of the gated cells of interest.

Table 2. Flow cytometer settings LIVE/DEAD near infrared analysis

Detector	Laser	Emission filter (nm/BP)	Fluorophore	Antibody conjugation
FL1	488 nm	533/30	FITC (green)	Anti-CD3
FL2	488 nm	585/40	-	-
FL3	488 nm	670/LP	-	-
FL4	640 nm	780/60	Dye (near-IR)	-

BP: Band Pass width. LP: Long Pass. FITC: Fluorescein isothiocyanate. Near-IR: near infrared.

6. Microscopical analysis of cell viability

Leukocyte morphology and immunofluorescent labeling were microscopically examined (Eclipse Ti-E, Nikon Instruments Europe B.V.) after Annexin-V FITC/PI labeling. Leukocytes were concentrated onto microscope slides via cytospin (Suppl. Procedure II). Data obtained was processed using NIS-Elements AR software (v. 4.00.02). Cellular morphology was visualized using phase/contrast microscopy and detected in the standard DIC-channel, whereas blue, green and red epifluorescent emission light was detected in the DAPI-, GFP-, and TRITC-channel, respectively (Table 3).

Table 3. Microscopy settings Annexin V/PI analysis

Channel	Light	Used label	Visualization
DIC	Phase/contrast	-	Morphology
Channel	Fluorescence	Used label	Visualization
DAPI	Blue	DAPI	Nucleic acid
GFP	Green	Annexin V-FITC	Phosphatidylserine
TRITC	Red	PI	Nucleic acid

DIC: Differential interference contrast. DAPI: 4',6-diamidino-2-phenylindole. GFP: Green Fluorescent Protein. TRITC: Tetramethylrhodamine. FITC: Fluorescein isothiocyanate. PI: Propidium Iodide

7. *In vitro* Delayed-Type Hypersensitivity assay

Under aseptic conditions, aliquots of WB were diluted with an equal volume of RPMI (Gibco), supplemented with stimulants (i.e. challenges). Subsequently, assay volumes of 1.5 ml were transferred into 1.0 ml cryotubes (NUNC). The assay tubes consisted of WB diluted with; **a)** RPMI only (i.e. negative control), **b)** RPMI and bacterial recall antigens (i.e. diphtheria-, tetanus- and pertussis-toxoid combined in a 1% Boostrix vaccine; GlaxoSmithKline, Rixensart, Belgium), **c)** RPMI in combination with monoclonal anti-CD3, anti-CD28 antibodies (10 µg/ml) (BD), or **d)** 0.5% pokeweed mitogen (PWM; Sigma-Aldrich Chemie GmbH, Steinheim, Germany) as positive control. The assay tubes containing the different mixtures were incubated for 24 h at 37°C, under *1 x g* or s-µG using the RPM (Fig. 6). At the 24 h time-point, 800 µl of the supernatant was collected into 1.5 ml Eppendorf tubes after 15 min centrifugation at *1500 x g*. Tubes were immediately frozen at -80°C until further processing.

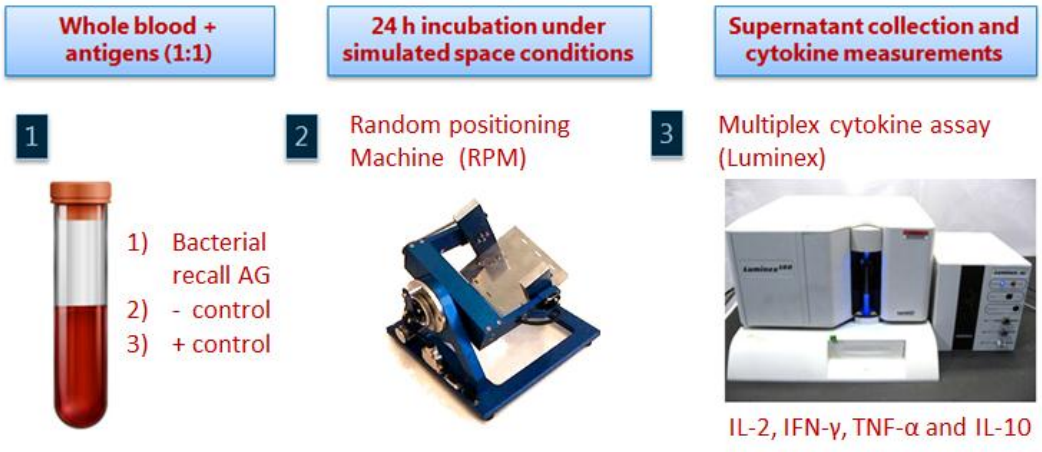

Figure 6. Scheme of the *in vitro* Delayed-Type Hypersensitivity assay.

In a second phase, the potential effect of stress hormone addition (i.e. psychological stress simulation) on the cell-mediated cytokine response was studied using the *in vitro* DTH assay with minor modifications (Table 4). Following blood collection, aliquots of WB were initially treated (i.e. pre-challenge) with varying concentrations of HC (Solu-Cortef®, Pharmacia and Upjohn Company, Pfizer, NY, USA) stress hormone (i.e. 0-600 ng/ml WB) and placed on a rocking platform for 6 h (*1 x g*). After this 6 h pre-challenge incubation time point, plasma was collected for cytokine analysis and remaining HC-treated WB was used as starting material for the *in vitro* DTH assay.

Table 4. Set-up of the *in vitro* DTH assay in combination with stress simulation

Hydrocortisone (HC) (ng/ml WB) [1] 0 [2] 100 [3] 200 [4] 400 [5] 600	→	**6 h incubation** ***1 x g***	MEASURING	**Addition challenges** ▪ Basal ▪ 1% Boostrix ▪ 10 µg/ml anti-CD3/CD28 ▪ 0.5% PWM	→	**24 h incubation s-µG**, 37°C **24 h incubation** ***1 x g***, 37°C	MEASURING

HC: Hydrocortisone. *1 x g*: Earth's gravity. s-µG: simulated microgravity. PWM: Pokeweed mitogen. Measuring: plasma collection and cytokine measurement. Whole blood (WB) aliquots are incubated for 6 h with HC. Mid-assay plasma collection is performed for each HC-condition. Afterwards remaining HC-treated WB is transferred into cryotubes and diluted (50%) with RPMI containing a specific challenge. Closed tubes are incubated for 24 h under *1 x g* or s-µG, and analyzed.

8. Assessment of inflammatory cytokine production

After performing the DTH assay, data on the immune response was collected by measuring changes in concentrations of multiple cytokines, which are known to be involved in the CMI response. After thawing of frozen plasma samples, the concentrations of both pro-inflammatory T helper type 1 (Th1)-cytokines (IL-2, IFN-γ and TNF-α) and anti-inflammatory Th2-cytokine (IL-10), were measured simultaneously by Luminex® technology (Suppl. Procedures III), according to the manufacturer's guidelines using the MILLIPLEX® MAP Human Cytokine/Chemokine kit (Merck Millipore, Merck KGaA, Darmstadt, Germany). The cytokine concentration detection limit was 2-10000 pg/ml and data was analyzed using xPONENT (build 3.1.971.0) software.

9. Statistical analysis

Statistical differences between the mean percentage of viable leukocytes were statistically determined via one-way analysis of variance (ANOVA), followed by Bonferroni's post-hoc test using GraphPad Prism (GraphPad Software Inc., version 5.01). Statistical significance was reached for p-values less than 0.05.

III. Results

1. Optimization viability assessment

In the first objective of my thesis, we aimed at investigating whether the applied experimental setup regarding the use of closed tubes during µG-simulation, could potentially influence the viability of immune cells.

1.1. Effects blood dilution and selective hypotonic red blood cell lysis

First, possible interfering factors such as WB dilution (50% v/v WB in RPMI; Fig. 7) and RBC lysis procedure (Fig. 8) on general leukocyte population distribution (i.e. FSC-A/SSC-A plot) were analyzed using flow cytometry.

Flow cytometric analysis of WB or DB (Fig. 7) after samples had been incubated for 24 h at 37°C at Earth's gravity (*1 x g*; Fig. 1A-B), or under µG-simulation (Fig. 1D-E) indicated that leukocytes were similarly distributed among the FSC-A/SSC-A plot for all test conditions, with varying background signal due to platelet contamination and cellular debris (i.e. FSC-A low events inside red boxes).

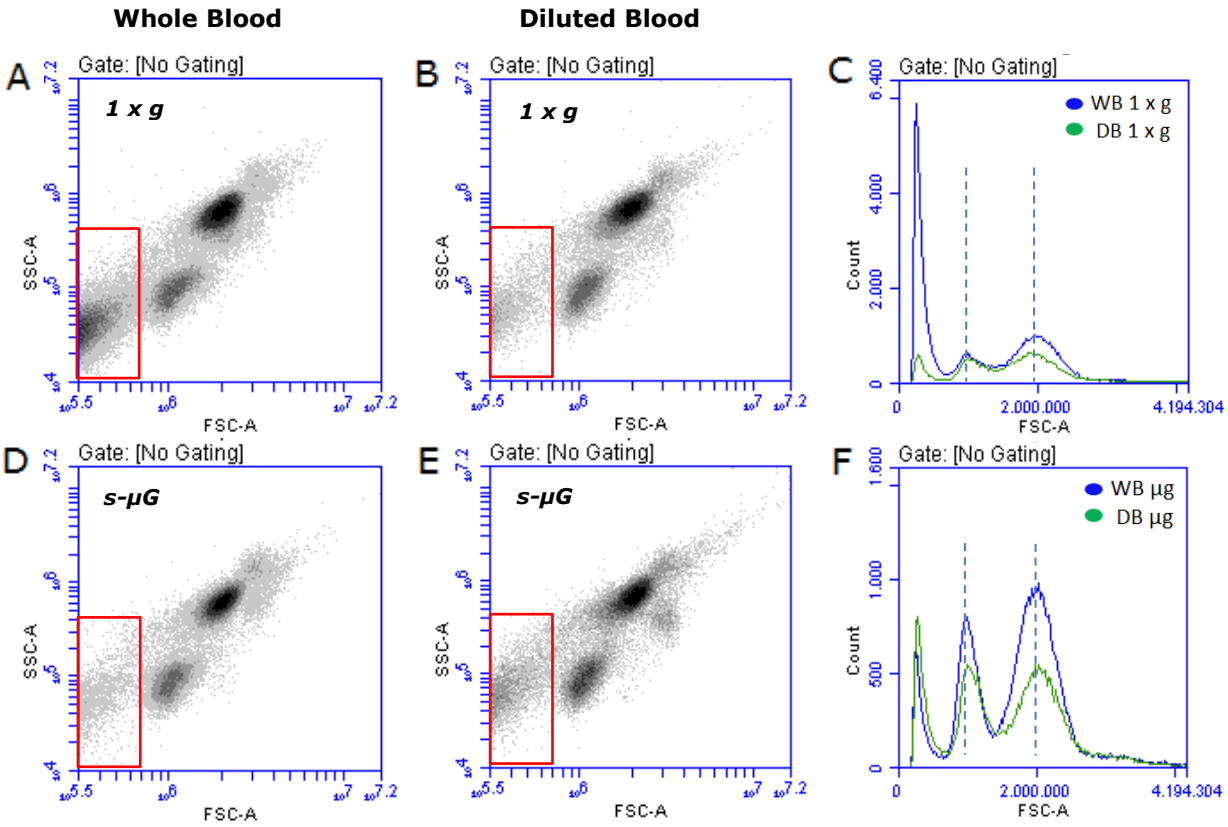

Figure 7. Flow cytometric analysis of FACS-isolated leukocytes from whole or diluted peripheral blood. FSC-A/SSC-A plots of **(A)** whole blood (WB) and **(B)** diluted blood 50% v/v WB in RPMI (DB), incubated at Earth's gravity (*1 x g*) for 24 h at 37°C. **C)** Count plot comparing FSC-A signal (i.e. cell size) of plots displayed in A-B, showing an equivalent mean FSC-A value (vertical dashed lines) for WB and DB. The first high WB (blue) count peak correlates to high background signal (red box). FSC-A/SSC-A plots of **(D)** WB and **(E)** DB, incubated under simulated microgravity (s-µG) on the RPM in 3D Random Mode for 24 h at 37°C. **F)** Count plot comparing cell size of plots displayed in D-E, indicating an equivalent mean FSC-A value (vertical dashed line) for WB and DB. Red boxes enclose background signal. FSC-A: Forward Scatter-Area, SSC-A: Side Scatter-Area

Furthermore, count plots displaying FSC-A characteristics (i.e. cell size) showed evenly distributed peaks along the FSC-A axis (i.e. no shift in cell size) between *1 x g* (Fig. 1C) and s-µG (Fig. 1F). This data indicates that diluting WB with RPMI does not induce changes in general leukocyte distribution. Therefore, future experiments will be performed using $DB_{1:2}$ (i.e. less viscous), which will in turn facilitate downstream applications (e.g. *in vitro* DTH assay).

In advance to immunofluorescent Annexin V/PI labeling, peripheral blood leukocytes were purified from contaminating RBCs using different selective hypotonic RBC lysis solutions. Potential confounding effects of FACS, or Promega lysing solutions on leukocyte population distribution (i.e. FSC-A/SSC-A plot), were analyzed after 24 h of incubation at 37°C under *1 x g* or s-µG (Fig. 8). Background signal (i.e. red boxes) on FSC-A/SSC-A dot plots were markedly increased after treatment with Promega Lysis solution (Fig. 8B, E), compared to FACS lysing solution (Fig. 8A, D). Furthermore, the use of Promega lysing solution (red graph line, induced a distinct shift in FSC-A of the cell populations to the right (i.e. increase in cell size) in both *1 x g* (Fig. 8C), as well as s-µG (Fig. 8F) compared to samples treated with FACS lysis (black graph line). This data suggests that RBC lysis using FACS lysing solution is more efficient in removing RBCs from the blood (i.e less background) compared to the Promega lysis solution.

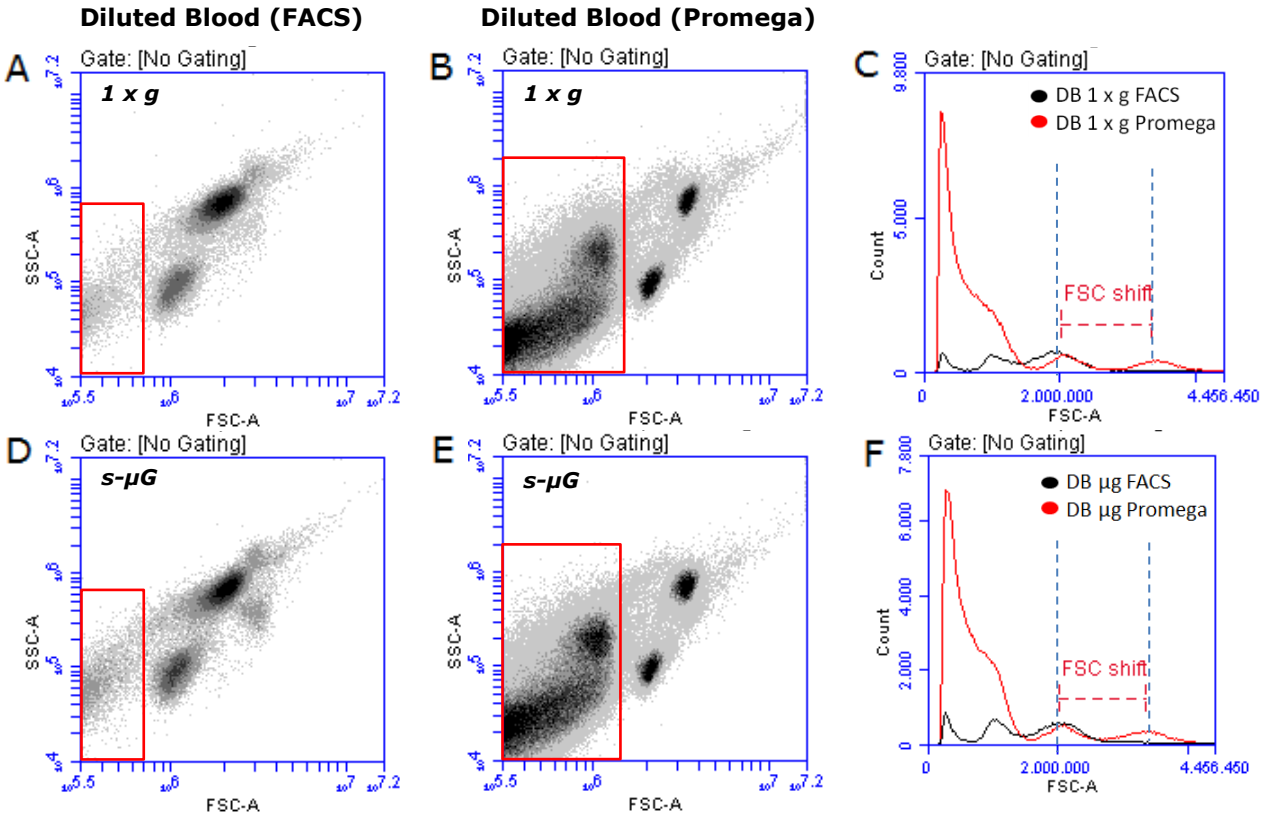

Figure 8. Flow cytometric analysis of diluted peripheral blood after different red blood cell lysis procedures. FSC-A/SSC-A plots of diluted blood (DB; 50% v/v WB in RPMI), incubated at Earth's gravity (*1 x g*) for 24 h at 37°C, and treated with FACS **(A)**, or Promega **(B)** red blood cell (RBC) lysing solution. **C)** Count plot comparing FSC-A signal (i.e. cell size) of plots displayed in A-B, showing a shift in mean FSC-A value (vertical dashed lines) between FACS and Promega RBC lysis conditions. The first high (red) count peak correlates to high background signal of Promega treated samples (red boxes). FSC-A/SSC-A plots of DB treated with FACS **(D)**, or Promega RBC lysis **(E)**, incubated under simulated microgravity (s-µG) on the RPM in 3D Random Mode for 24 h at 37°C. **F)** Count plot comparing cell size of plots displayed in D-E, indicating an equivalent shift in mean FSC-A value (vertical dashed line), as seen in C. Red boxes enclose background signal. FSC-A: Forward Scatter-Area, SSC-A: Side Scatter-Area

1.2. Annexin V/PI labeling after FACS red blood cell lysis

Aliquots of $DB_{1:2}$ were labeled with monoclonal anti-CD45 antibodies (i.e. leukocyte-specific marker) conjugated to APC and RBCs were lysed with FACS lysing solution. Samples were finally labeled with Annexin V/PI to assess leukocyte viability using flow cytometry. Analyses were performed at 0 h (i.e. pre-incubation control, Fig. 9A, D) and after 24 h of incubation under *1 x g* (Fig. 9B), or s-µG (Fig. 9C). Panels (A-C) show ungated dot-plots displaying CD45 and SSC characteristics of all collected events. Accordingly, leukocytes were gated by enclosing the CD45-APC positive events (panels D-F). Dot-plots (A-C) were similar between time points as well as gravity conditions, and leukocyte percentages ranged from 65.9-70.6% of all collected events. Flow cytometric data of the viability plots (D-F) showed that nearly all leukocytes were positive for PI (i.e. marker for dead cells), independent from analysis time point or gravity condition.

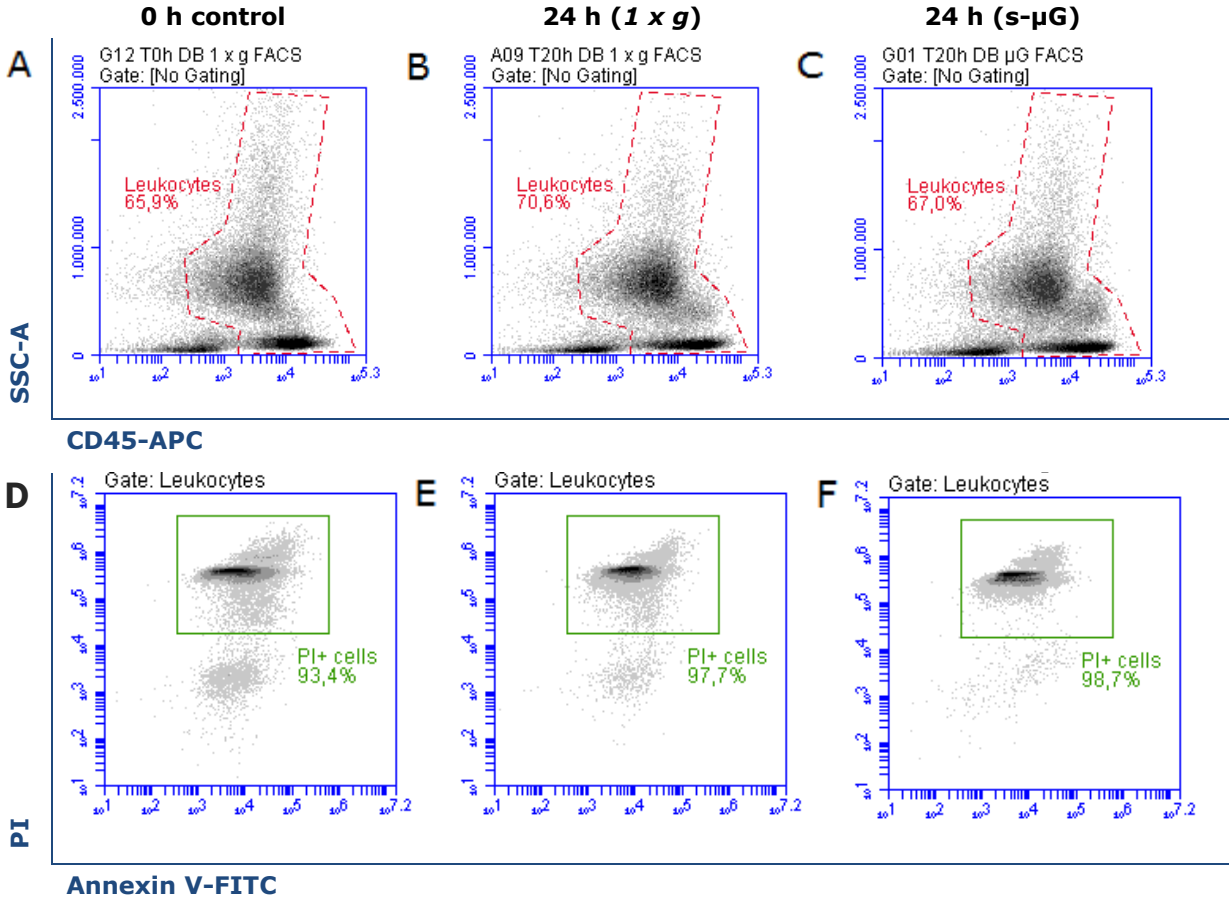

Figure 9. Identification and viability labeling of isolated leukocytes. Diluted Blood (DB) was processed before incubation **(A)** or after 24 h-incubation under *1 x g* **(B)** or s-µG **(C)**. Purified leukocytes underwent, labeling with monoclonal anti-CD45-APC antibodies, red blood cell lysis (FACS) and Annexin V/PI viability labeling. Leukocytes were gated based on dot plots **(A-C)** displaying CD45 and side scatter (SSC) properties of the collected events. Viability plots **(E-F)** displaying Annexin V-FITC and Propidium Iodide (PI) signals of the collected events inside the leukocyte gatings (A-C). Green boxes enclose PI^+ proportion (i.e. dead cells) of the gated leukocytes.

1.3. Microscopical validation of Annexin V/PI labeling

The basic morphology (i.e. cell shape) of leukocytes was microscopically examined for both FACS or Promega-treated DB samples after Annexin V/PI labeling. Phase-contrast imaging of a blood sample treated with FACS lysis, showed circular-shaped leukocytes with seemingly intact cell membranes (Fig. 10A). In contrast, blood samples treated with Promega lysing solution showed degranulated leukocytes which completely lack membrane integrity (Fig. 10B).

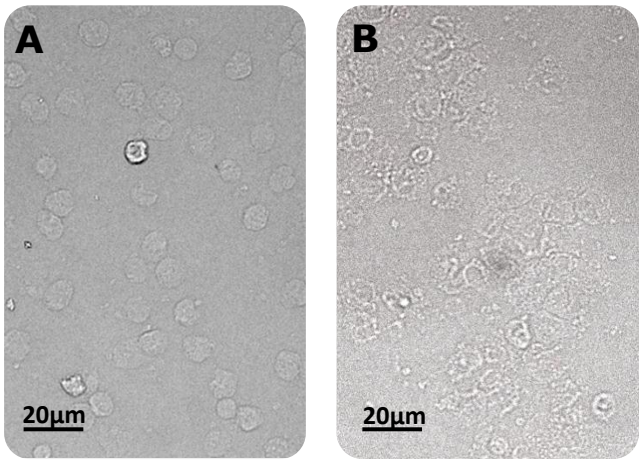

Figure 10. Phase contrast images displaying leukocyte morphology. Leukocytes are displayed after FACS lysis (A), or Promega lysis (B) of RBCs, viability labeling and cytospin onto microscope glasses. Scale bars = 20 µm.

Immunofluorescent labeling was microscopically examined as well (Fig. 11), using isolated leukocytes after 24 h of incubation under normal gravity (*1 x g*). Leukocyte nuclei were counterstained with DAPI (Fig. 11A) showing a typical mix of circular (i.e. lymphocytes, monocytes) and granular-shaped nuclei (i.e. granulocytes). The expression of PS (i.e. marker for early apoptosis) on the outer cell membrane was visualized (white arrows, Fig. 11B) through specific targeting and binding with FITC-labeled Annexin V antibodies. Late apoptotic and necrotic cells were distinguished from early apoptotic cells (i.e. still viable cells) using PI labeling (Fig. 11C). Microscopical data corresponded with flow cytometric data (i.e. see Fig. 11B, lower panel), showing an almost complete number of PI^+ leukocytes due to the inducement of cell membrane permeabilization by the formaldehyde component of the FACS lysis solution.

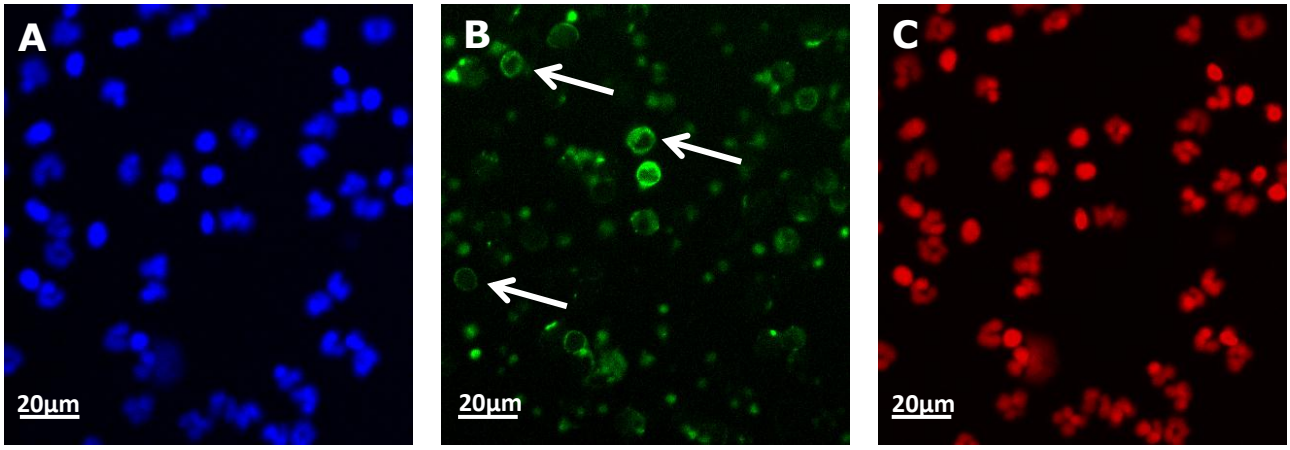

Figure 11. Immunofluorescent viability labeling of leukocytes. Leukocytes were incubated (*1 x g*) for 24 h, purified from RBCs using FACS lysis and subsequently labeled with Annexin V-FITC **(B)**, PI **(C)** and DAPI **(A)** as nuclear control stain. Displayed pictures are taken of the same sample and position, but using different detection channels. White arrows in B indicate Annexin V labeling on the outside of the cellular surface. Scale bars = 20 µm.

2. Peripheral blood mononuclear cell isolation

Due to the incompatibility of using RBC lysis solutions which contain membrane permeabilizing fixatives, PBMC isolation was applied as an alternative mononuclear leukocyte purification method (Fig. 12). PBMCs were isolated from 3ml $DB_{1:4}$ (i.e. contains 0.75 ml WB) by density gradient centrifugation at 0 h (Fig. 12B), and after 24 h of incubation at *1 x g* (Fig. 12C), or s-µG (Fig. 12D). The MNC layer (Fig. 12B, red marked region) resides in the transfer zone separating the transparent Histopaque and the yellow blood plasma. PBMC isolation after 24 h incubation in *1 x g* yielded a slightly red-toned Histopaque medium (Fig. 12C), indicating a suboptimal blood fractionation.

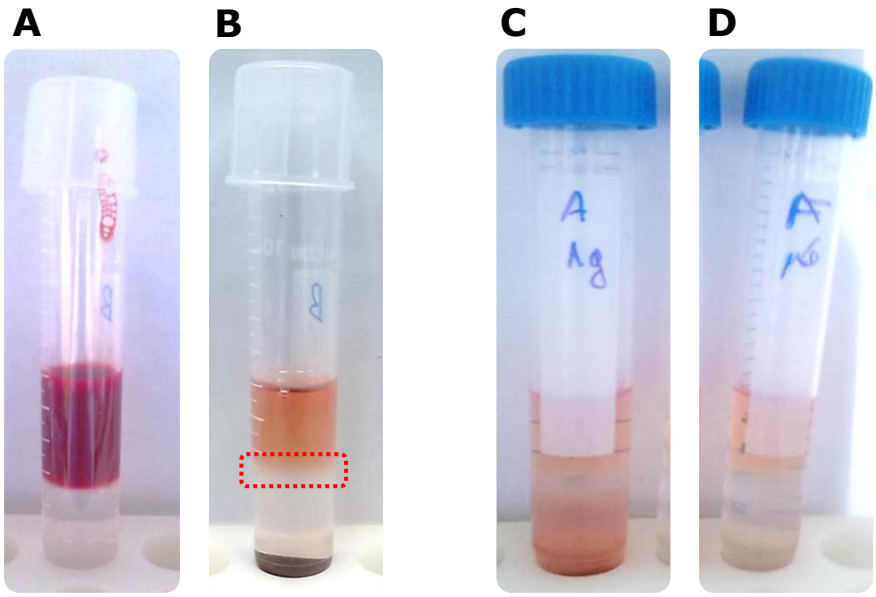

Figure 12. Peripheral blood mononuclear cell isolation. **A)** Centrifuge tube with 3 ml $DB_{1:4}$ pipetted on top of the transparent histopaque medium. **B)** Fractionated blood after centrifugation of 0 h control sample. Transparent layer of Histopaque is separated from orange blood plasma layer on top by a mononuclear cell layer (i.e. buffy coat in red marked region). RBCs and granulocytes sediment towards the bottom. **C)** Fractionated blood after 24 h of incubation in closed tubes at *1 x g*. **D)** Fractionated blood after 24 h of microgravity-simulation in closed tubes.

2.1. Annexin V/PI labeling of peripheral blood mononuclear cells

Following blood collection (0 h), isolated PBMCs (n=2) were labeled with monoclonal anti-CD45 antibodies conjugated to APC. Subsequently, leukocyte viability was examined using the Annexin V-FITC apoptosis detection kit (eBioscience). During flow cytomteric analysis, PBMCs were gated (Fig. 13A) and displayed in corresponding viability plots (Fig. 13B), based on the Annexin V-FITC and PI signals of the gated PBMCs. Additionally, the viable (green Annexin V^-/PI^- gate), early apoptotic (blue Annexin V^+/PI^- gate) and unviable (red Annexin $V^{(-/+)}/PI^-$ gate) cell population were gated (Fig. 13B). Data analysis showed that at 0 h, 69.48 ± 1.79% of total PBMCs were viable (i.e. green column Fig. 13C), 24.58 ± 1.21% were early apoptotic (i.e. blue column Fig. 13C) and 6.12 ± 0.68% were unviable (i.e. red column Fig. 13C).

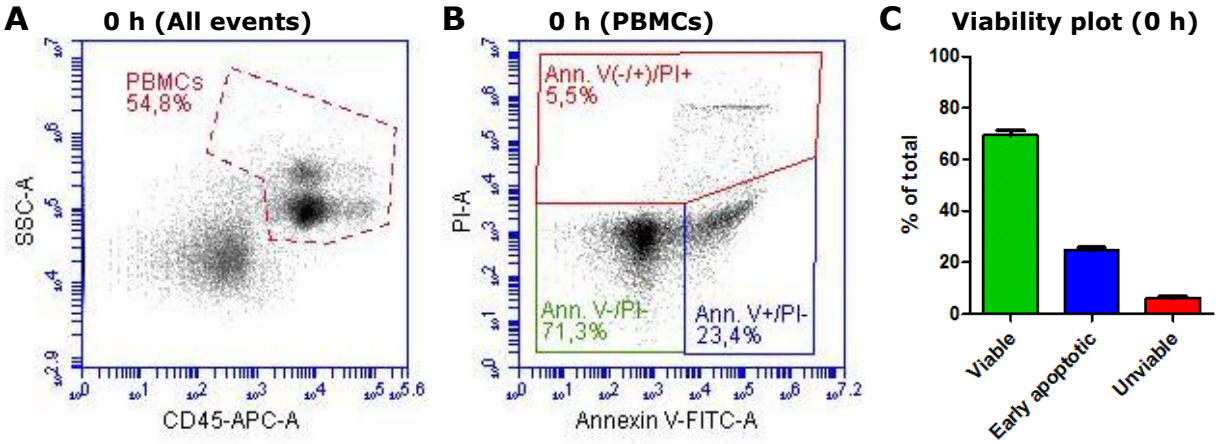

Figure 13. Viability labeling and gate placement on dot plot of sample immediately processed after blood collection (0 h). **A)** PBMC gate placement. **B)** Viability plot of gated PBMCs of (A) displaying additional colored gates for viable (i.e. green Annexin V^-/PI^- gate), early apoptotic (i.e. blue Annexin V^+/PI^- gate) and unviable (i.e. red Annexin $V^{(-/+)}/PI^-$ gate) cell populations. **C)** Viability plot in bar-graph format of (B), showing the fraction (%) of each viability subset before starting incubation. *Representative donor is shown for A, B.* (C; n=2, mean ± SEM)

The effect of time (i.e. 24 h incubation in closed cryotubes), as well as the consequence of gravitational changes (i.e. µG-simulation) on the viability of isolated PBMCs (n=2) were studied (Fig. 14). Using the Annexin V/PI labeling, the mean percentage of viable, early apoptotic and unviable PBMCs neither varied markedly between 0-24 h, or between *1 x g* or s-µG incubation. However, no statistical analysis could be performed due to the small sample size.

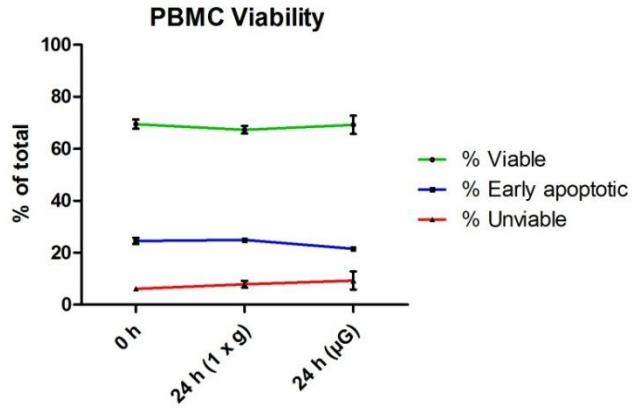

Figure 14. PBMC viability at 0-24 h of incubation under normal or simulated microgravity. Viability was assessed after blood collection (0 h control) and after 24 h of incubation under normal gravity (*1 x g*), or simulated microgravity (s-µG). The mean viable (green line), early apoptotic (blue line) and unviable (red line) fraction (%) of total PBMCs are displayed for each time-point on the x-axis. n=2, mean ± SEM

3. LIVE/DEAD assay using fluorescent amine-reactive labeling

After PBMCs (n=6) were isolated from $DB_{1:4}$ (0 h), cells were labeled with near-infrared fluorescent dye (LIVE/DEAD® Fixable Dead Cell Stain Kits, Invitrogen). Subsequently, PBMCs were labeled with monoclonal anti-CD3-FITC antibodies (i.e. investigate T cell viability) and cells were fixed. During flow cytometric analysis background events were gated (Fig. 15A) and excluded. The remaining PBMCs were plotted and the $CD3^+$ population (i.e. T cells) was gated, based on the intensity of the CD3-FITC signal (Fig. 15B). The percentage of viable (i.e. LIVE gate), or dead T cell population (i.e. DEAD gate) is shown in a count plot displaying the fluorescent near-infrared signals of the gated $CD3^+$ T cells (Fig. 15C).

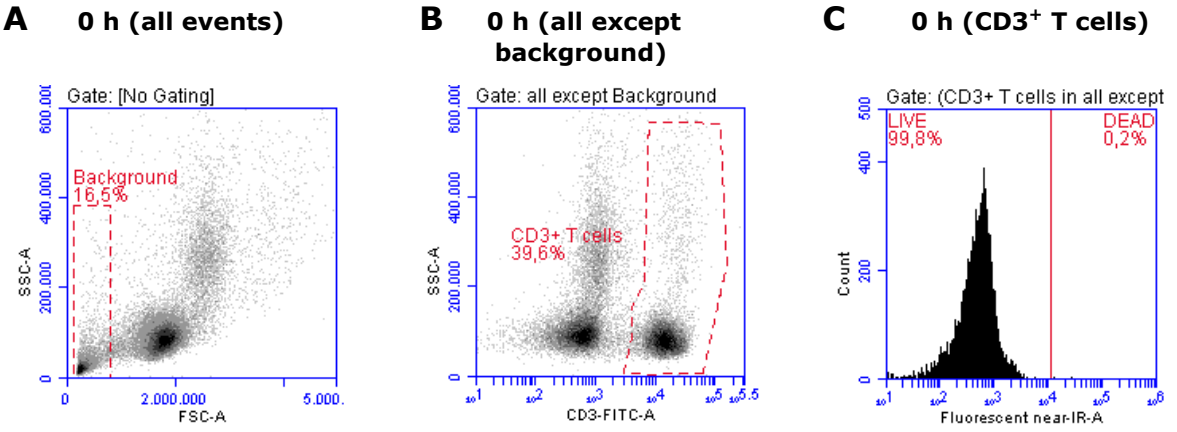

Figure 15. LIVE/DEAD fluorescent near-infrared labeling following blood collection (0 h) and gate placement for T cells. **A)** Background gating on dot-plot displaying all collected events, used to exclude non-cellular events. **B)** Gating of the $CD3\text{-}FITC^+$ T cell population. **C)** Count plot displaying fraction (%) of viable (LIVE) or unviable (DEAD) T cells at 0 h (control) time point. Representative donor is shown in A-C.

Following blood collection (0 h) 99.60 ± 0.08% of gated T cells were viable. Dot-plots displaying the gated $CD3\text{-}FITC^+$ T cell populations of samples incubated for 24 h under normal gravity (*1 x g*, Fig. 16A), s-µG (Fig. 16B) and normal gravity with 10 µM staurosporine (i.e. positive control Fig. 16C). Additionally, corresponding count plots displaying the percentage of viable (i.e. LIVE-gate) and unviable (i.e. DEAD-gate) are shown for *1 x g* (Fig. 16D), s-µG (Fig. 16E) and positive control (Fig. 16F).

The mean viable percentage of total gated $CD3^+$ T cells is displayed in Fig. 17 for donor-matched samples, analyzed before (0 h) and after incubation (24 h) under normal gravity (*1 x g*) or s-µG. Pre-incubation analysis showed that 99.60 ± 0.08% of gated T cells were viable at the 0 h control time-point. In contrast, post-incubation analysis after 24 h of incubation under *1 x g* or s-µG, respectively indicated that 95.39 ± 0.47% and 95.96 ± 1.32% of T cells were still viable. Statistical one-way analysis of variance (ANOVA) showed an overall significant difference between the groups ($p=0.0044$). Moreover, post-hoc Bonferroni's multiple comparison tests indicated a significant decrease in the mean percentage of viable T cells after 24 h under *1 x g* ($p<0.01$) and s-µG ($p<0.05$), compared to 0 h controls. No difference in mean T cell viability was found between the *1 x g* and s-µG post-incubation groups.

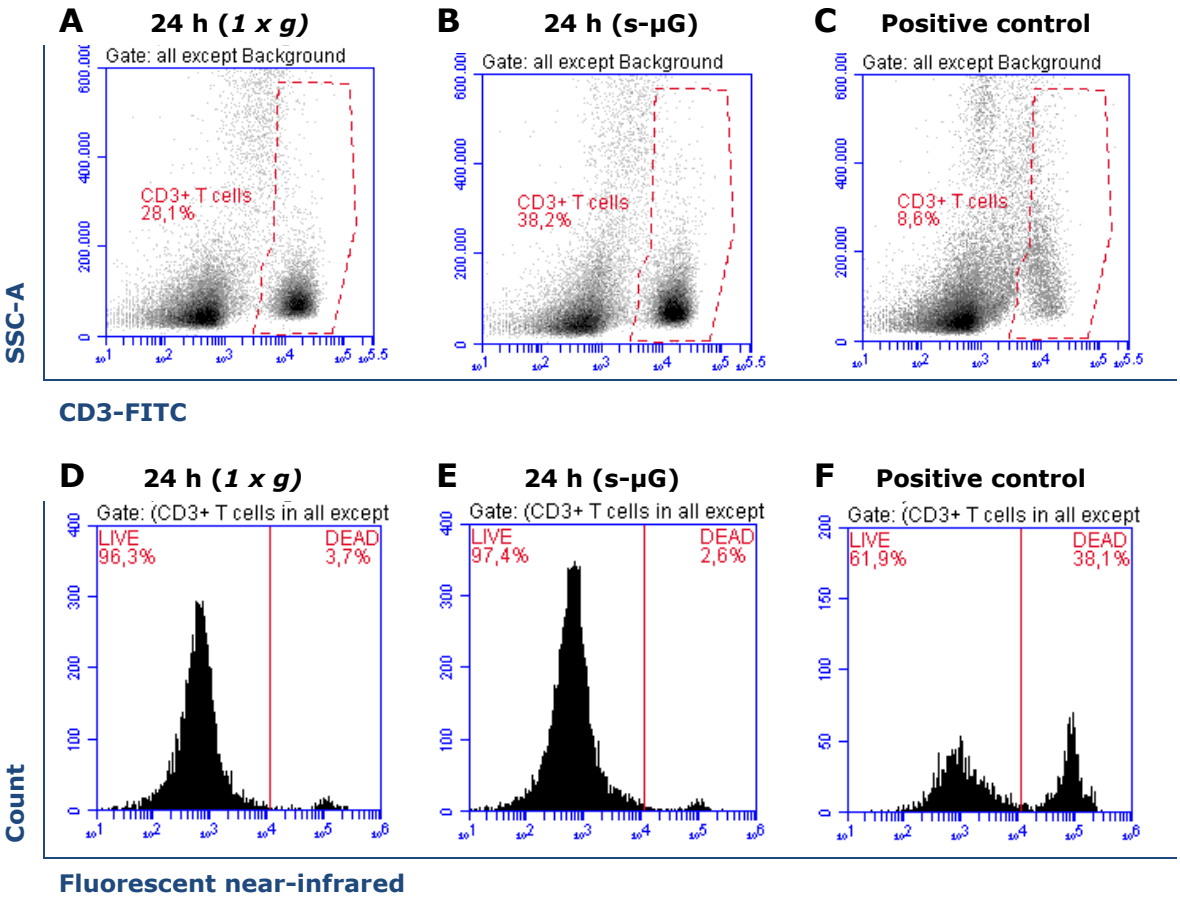

Figure 16. LIVE/DEAD fluorescent near-infrared labeling after 24 h of incubation under normal or simulated µG. Dot-plots displaying the gated CD3-FITC$^+$ T cell populations of sample incubated for 24 h under normal gravity (*1 x g)* **(A)**, s-µG **(B)** and normal gravity with 10 µM staurosporine **(C)** which is used as positive control. Count plots **(D-F)** displaying the fraction (%) of viable (LIVE) and unviable (DEAD) CD3-FITC$^+$ T cells. Plot D, E and F match with plot A, B and C, respectively. Representative donor is shown in A-F.

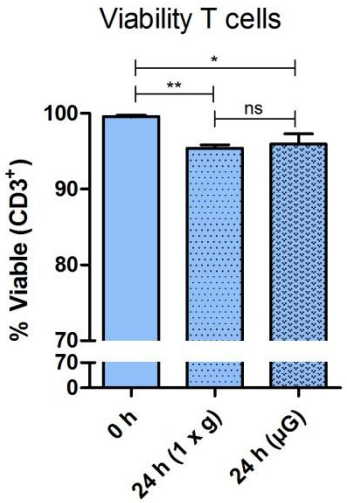

Figure 17. Fraction of viable T cells after 24 h of incubation under normal or simulated µG. The mean fraction (%) of viable CD3$^+$ cells was significantly lower after 24 h of incubation under normal (*1 x g*) or simulated microgravity (s-µG), for donor-matched samples compared to 0 h controls. Gravity incubation-type (*1 x g* vs. s-µG) did not yield significant changes in T cell viability. n=6, mean ± SEM. ** P value < 0.01; * P value < 0.05; ns not significant. Used statistics: One-way ANOVA with Bonferroni's post-hoc test.

4. Evaluation of the cell-mediated immune response *in vitro*

4.1. Effects of simulated microgravity on cytokine response

The individual impact of 24 h of µG-simulation on plasma levels of pro- (IFN-γ, IL-2, TNF-α) and anti-inflammatory (IL-10) cytokines, was investigated using the *in vitro* DTH assay followed by multiplex cytokine analysis. Immune cells were stimulated and activated using different challenges and the evoked cytokine levels were compared to basal cytokine levels of unchallenged control samples. The differential response of each cytokine in function of the used challenge is shown in Fig. 19. Plasma IFN-γ levels (Fig. 19A) were highest after T cell stimulation with monoclonal anti-CD3 and anti-CD28 antibodies and levels were similar between s-µG and *1 x g*. However, stimulation with bacterial recall antigens showed decreased IFN-γ levels under s-µG compared to *1 x g*. Basal plasma IL-2 levels were below detection limit (Fig. 19B). Stimulation with bacterial recall antigens elicited a rise in plasma IL-2 under *1 x g*. However, under s-µG the IL-2 response to stimulation is completely blunted (Fig. 19B). In contrast, anti-CD3 and anti-CD28 antibodies yielded an inverse response. After µG-simulation, higher IL-2 concentrations were measured compared to control samples. Plasma levels for IL-10 (Fig. 19C) and TNF-α (Fig. 19D) were markedly elevated after stimulation of the lymphocyte population (i.e. T and B cells) with PWM compared to basal levels.

Each specific type of challenge induced a varied cytokine response profile for the different cytokines (Fig. 20). Bacterial recall antigens (diphtheria-, tetanus- and pertussis-toxoids) of the Boostrix vaccine (Fig. 20A) showed an inhibited response under s-µG for all cytokines compared to *1 x g*, except for IL-10 which did not respond. Stimulation with monoclonal antibodies (Fig. 20B) resulted in a high IFN-γ and TNF-α response, seemingly unaffected by s-µG. However, basal IFN-γ and TNF-α levels were slightly decreased under s-µG compared to *1 x g*. In contrast, the IL-2 response after antibody-mediated stimulation was higher under s-µG (Fig. 20B). Immune cell stimulation with the plant lectin PWM only induced a notable response for IL-10 and TNF-α compared to unchallenged controls (Fig. 20C). After PWM stimulation, these cytokines showed a minor increase in plasma levels under s-µG compared to *1 x g*.

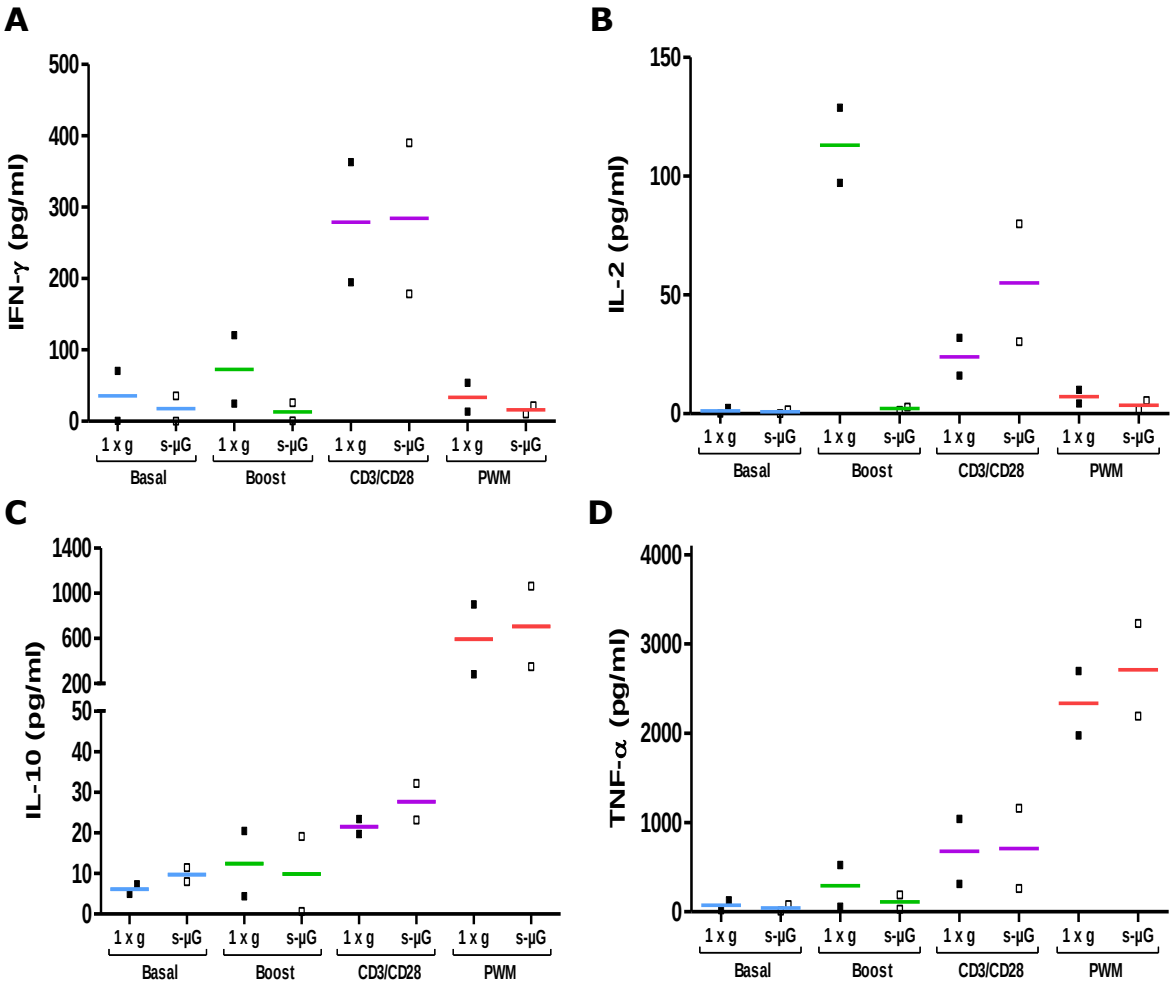

Figure 19. Mean cytokine response in function of used immunogenic challenge under simulated microgravity (s-µG) alone. Plasma levels are shown for **(A)** interferon gamma (IFN-γ), **(B)** interleukin 2 (IL-2), **(C)** interleukin 10 (IL-10) and **(D)** tumor necrosis factor alpha (TNF-α) after multiplex cytokine measurement (Luminex). *1 x g*: Earth's gravity. Basal: no addition of challenge. Boost: Bacterial recall antigen mixture of Boostrix vaccine. CD3/CD28: Monoclonal mouse anti-CD3, anti-CD28 antibodies. PWM: Pokeweed mitogen. (n=2; mean)

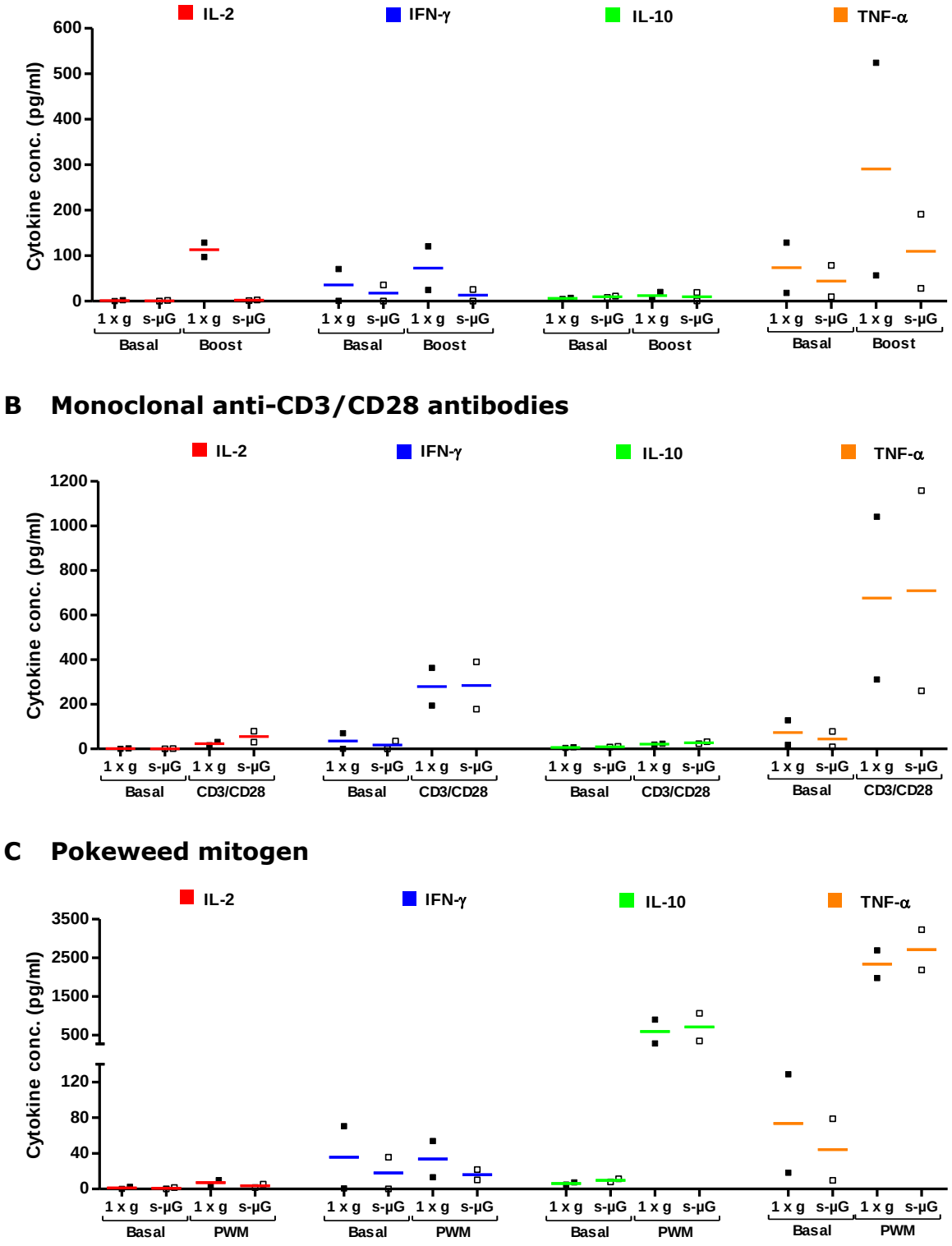

Figure 20. Plasma cytokine profile per specific challenge. (A) Boostrix vaccine bacterial recall antigens (Boost). **(B)** Monoclonal mouse anti-CD3 and anti-CD28 antibodies (CD3/CD28). **(C)** Pokeweed mitogen (PWM). Basal and induced cytokine response under Earth's gravity (*1 x g*) and simulated microgravity (s-µG) of interleukin 2 (IL-2), interferon gamma (IFN-γ), interleukin 10 (IL-10) and tumor necrosis factor alpha (TNF-α) are displayed. (n=2; mean)

4.2. Combined effect of simulated microgravity and stress hormones

The cytokine levels of IFN-γ, IL-2, IL-10 and TNF-α in the plasma of peripheral blood samples (n=2) were assessed after 6 h incubation under *1 x g* with varying concentrations of HC (i.e. corresponding to different states of mental stress). Results (Fig. 18) indicated that stress hormones alone did not induce pronounced cytokine responses of naive (i.e. non-stimulated) immune cells under normal gravity. Although a small rise in TNF-α concentration is visible from 0-100 ng/ml HC, the TNF-α response did not change (i.e. plateau formation) in function of further increasing HC concentrations. The measured cytokine levels of IFN-γ, IL-2 and IL-10 were below the lower detection limit of the used assay.

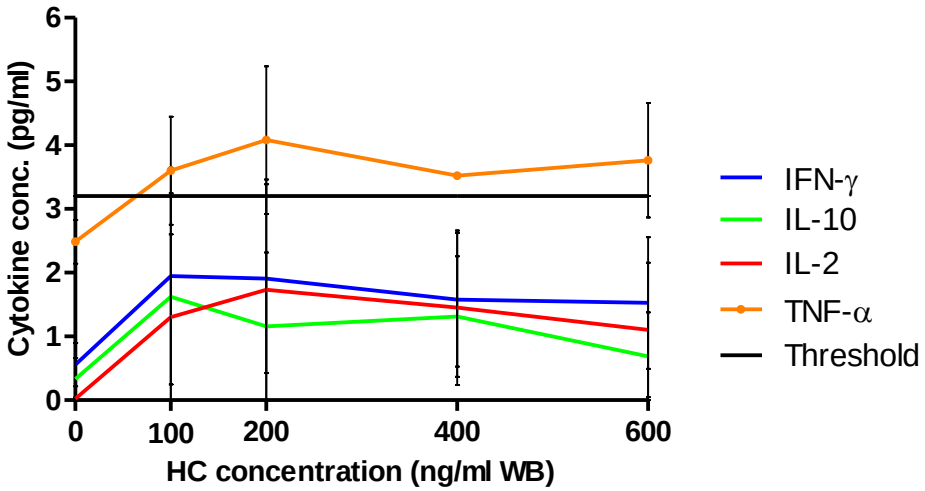

Figure 18. Plasma cytokine levels following a 6-hour hydrocortisone (HC) treatment under normal gravity. Plasma levels for interferon gamma (IFN-γ, blue), interleukin 2 (IL-2, red), interleukin 10 (IL-10, green) and tumor necrosis factor alpha (TNF-α, orange) are shown. The horizontal black line represents the lower detection limit 3.2 pg/ml. (n=2; mean ± SEM)

The impact of simulated mental stress in combination with s-μG on cytokine levels in the plasma was investigated by combining the standard *in vitro* DTH assay with stress homones. In short, immune cells prestimulated to stress hormones (HC), were further stimulated for 24 h under s-μG (3D RPM). The response of IFN-γ, IL-2, IL-10 and TNF-α under s-μG to different immunogenic challenges are displayed in function of the added concentration of HC (Fig. 21). The challenges are differentially colored; basal (Fig. 21A-D, green), bacterial recall antigens (Fig. 21E-H, blue), monoclonal anti-CD3/CD28 antibodies (Fig. 21I-L, yellow) and PWM (Fig. 21M-P, red). In addition, cytokine data points were taken from samples incubated under normal gravity (*1 x g,* dotted lines), or s-μG (solid lines). In the basal (i.e. non-stimulated) peripheral blood samples, only plasma IL-10 levels (Fig. 21C) displayed a rising trend in function increasing HC concentrations. Stimulation with bacterial recall antigens induced a notable downward trend in plasma IL-2 levels (Fig. 21F) under normal gravity. In addition, IFN-γ (Fig. 21E) also showed a minor decreased trend from 0-200 ng/ml HC and remained unchanged at the higher HC concentrations. Monoclonal anti-CD3/CD28 antibody stimulation yielded a higher cytokine response for all measured cytokines under s-μG compared to *1 x g*. Additionally, a reduced trend in plasma IFN-γ (Fig. 21I), IL-2 (Fig. 21J) and TNF-α (Fig. 21L) levels was displayed in function of increasing concentrations of HC. After PWM-mediated immune cell stimulation the measured cytokine responses showed that only plasma TNF-α (Fig. 21P) was decreased in function of rising levels of HC.

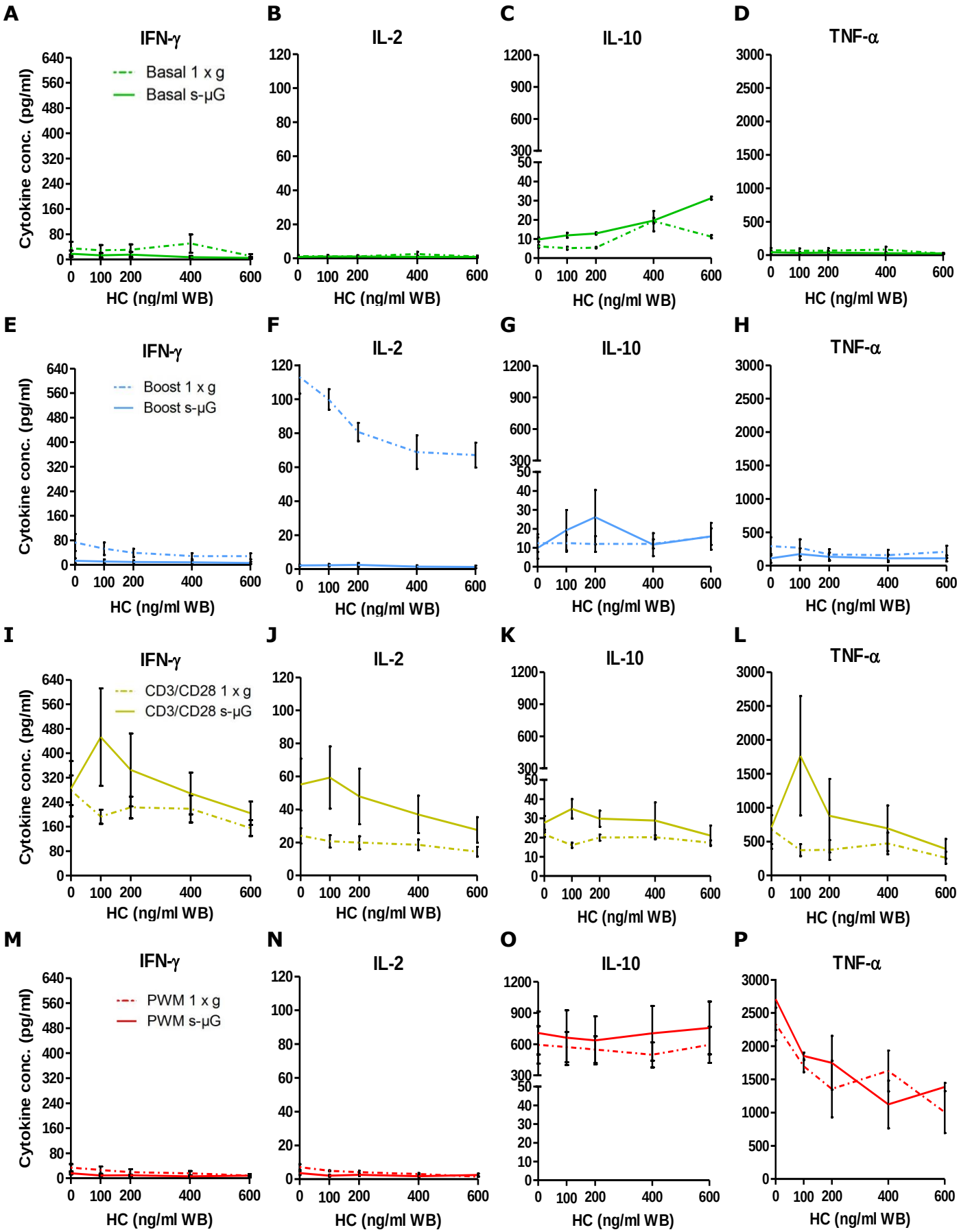

Figure 21. Effect of hydrocortisone in combination with simulated microgravity (s-µG) on cytokine response. Plasma IFN-γ, IL-2, IL-10 and TNF-α levels displayed in function of hydrocortisone (HC) concentrations. **(A-D)** Non-stimulated (basal, green). **(E-H)** Bacterial recall antigens (Boost, blue). **(I-L)** Monoclonal anti-CD3 and anti-CD28 antibodies (CD3/CD28, yellow). **(M-O)** Pokeweed mitogen (PWM, red). (n=2, mean ± SEM)

IV. Discussion and Outlook

Although it is clear that the astronaut's immune system is affected in space, it is still too early to definitively conclude that there is indeed a clinical risk associated with the dysregulation of the immune system during spaceflight. The main challenge is the difficulty to obtain human in-flight data of long-duration missions. Moreover, the collected data might potentially be skewed due to post-flight interferences such as stress caused by readaptation to Earth's gravity. In addition, the majority of real spaceflight data concerning the immunity in space has been extrapolated from short-duration missions which might not accurately reflect long-term immunological effects (35). Nonetheless, the collection of additional spaceflight data is crucial in order to fully unravel the underlying immune-modulative mechanisms associated with spaceflight.

In this project we attempt to obtain more information about the effects of spaceflight stressors on the immune system using ground-based *in vitro* spaceflight analogues. With the use of such models, reproducible Earth-based space research can be performed in preparation for immunology experiments in space such as MoCISS.

Assessment of leukocyte viability under simulated microgravity

The first objective of my thesis focused on verifying whether the applied experimental setup regarding the use of closed tubes on the RPM for simulating µG, could potentially induce changes in the viability of leukocytes. Underlying alterations in cell viability might confound the interpretation of future cytokine measurements. Therefore, the viability of leukocytes as well as the T cell-subset present in peripheral blood samples was analyzed after 0-24 h of incubation in closed tubes (i.e. requirement for MoCISS space-experiment) under *1 x g*, or s-µG. Initial experiments were performed using the Annexin V-FITC/PI assay in combination with preceding hypotonic RBC lysis. The assay is based on the detection of apoptotic markers on the outer cell membrane. Starting from the early stages of apoptosis, PS is translocated from the cytosolic side to the extracellular side of the cell membrane. The exposed PS is subsequently targeted using Annexin V, which is a phospholipid-binding protein with high affinity for PS. In contrast to the initial stages of apoptosis, the cell membranes become leaky due to loss of structural membrane integrity during the more advanced stages of apoptosis and necrosis (36). PI has a high affinity for nucleic acids and can only be taken up by dead cells having leaky cell membranes (i.e. non-permeable in case of viable cells). Thus, combining Annexin V with PI labeling, both early apoptotic and dead cells can be detected and distinguished from each other.

Optimization of the Annexin V-FITC/PI viability assay

During the optimization phase of this assay, the efficacy of RBC removal was compared for both FACS and Promega lysis solutions. Flow cytometric analysis of the purified leukocyte populations after FACS lysis, resulted in well-distinguishable sub-populations with a low amount of background events. Additionally, microscopical analysis revealed a typical morphology of the leukocytes. In contrast, although flow cytometric analysis of blood lysed with Promega lysis solution showed distinguishable leukocyte sub-populations, they displayed an abnormal morphology under the microscope.

Moreover, there was a substantial amount of debris present after flow cytometric analysis. This apparent insufficiency of RBC removal through Promega lysis (i.e. high amount of debris), could visually be confirmed via the observation of red-toned cell pellets during the procedure (data not shown). On the contrary, cellular pellets after FACS lysis displayed the typical opaque color of pelleted cells. Based on the abovementioned findings we concluded that FACS lysing solution was a suitable candidate to be used for RBC removal in succeeding viability experiments.

Unexpectedly, both flow cytometric and microscopical data on Annexin V/PI-labeled samples pre-treated with FACS lysis, showed that nearly the whole purified leukocyte population was dead (i.e. PI^+), independent from analysed time-point or gravity condition. Thus, the used procedure resulted in a global loss of membrane integrity, allowing PI to pass the cell membranes and interact with the DNA. The underlying cause was later attributed to the composition of the FACS lysis buffer (37), which contains 9.99% formaldehyde according to BD's Material Safety Data Sheet. This well-known fixative induces membrane permeabilization (i.e. false positive effect) and is therefore incompatible with the Annexin V/PI labeling (38).

In order to circumvent the RBC lysis step, PBMC isolation was performed as an alternative leukocyte isolation procedure. This technique enables fractionation of blood components and is based on a density gradient separation (39). During centrifugation, both the RBCs as well as the high-density granulocytes (e.g. neutrophils), sediment towards the bottom of the tube. In contrast, lymphocytes and monocytes (i.e. mononuclear cells) have lower densities in the medium and remain at the plasma/Histopaque interface to form the MNC layer.

Peripheral blood mononuclear cell viability under simulated microgravity

PBMC isolation after 24 h of incubation in cryotubes was associated with increased platelet contamination and was as expected less optimal compared to baseline isolations (i.e. at 0 h). Accordingly, we observed a trend that samples incubated under *1 x g*, but not under s-µG, showed a slightly red-toned coloration of the normally transparent Histopaque after centrifugation. However, this could be explained by the blood sedimentation of stationary samples (i.e. 24 h incubation under *1 x g*), whereas µG-simulation results in continuous mixing of the blood inside the cryotubes. Prolonged sedimentation of the blood in *1 x g* might stimulate platelet coagulation, which could in turn hinder PBMC isolation (40).

Nevertheless, Annexin V/PI labeling of isolated PBMCs showed consistent amounts of viable, early apoptotic and unviable cell percentages, seemingly unaffected by incubation-time and gravity. Moreover, already at baseline (0 h) relatively high percentages of early apoptotic (24.58 ± 1.21%) and unviable (6.12 ± 0.68%) cells were displayed after flow cytometric analysis. These findings suggest that the applied procedure is rigorous and could potentially stress the isolated cells. However, the observation that the percentages do not markedly change over time, nor between *1 x g* and s-µG, indicates that the viability of the PBMCs stayed stable. Nonetheless, the sample number (n=2) was too limited to draw conclusions confirmed by statistics.

Viability of T cells after microgravity-simulation

In the next step, specific attention was pointed towards the viability of T cells under s-µG. Feuerecker et al. showed that the production of IL-2, one of the key cytokines needed for the initiation of the antigen-dependent immune response, was blunted in CD3-depleted cell cultures (i.e. cultures lacking T cells). Moreover, intracellular IL-2 staining of comparable non-depleted cell cultures identified T cells as the main source of IL-2 cytokine production. Taken together, these findings indicate the importance of functional T cells in CMI (33). With the use of a fluorescent amine-reactive dye PBMCs were labeled and analyzed by flow cytometry. The LIVE/DEAD assay is based on the reaction of the fluorescent label with free cellular amines, located both on the cell surface, as well as in the cytoplasm. The reactive dye is excluded from viable cells having intact cell membranes, allowing binding of only the extracellular amines (i.e. low intensity signal). In contrast, dead cells having leaky cell membranes, take up the reactive dye which results in binding of both the internal and external cellular amines (i.e. high intensity signal)(41). Flow cytometric analysis enables discrimination of the live (low intensity) and dead (high intensity) populations.

T cell viability was analyzed (n=6) after 24 h of µG-simulation and incubation in closed cryotubes. Similar to the Annexin V/PI assay, PBMCs were isolated, labeled (fluorescent amine-reactive dye, anti-CD3-FITC) and analyzed by flow cytometry. A major advantage of the LIVE/DEAD fluorescent dye is that the reaction is irreversible, allowing fixation and stabilization of the labeled cells. T cell viability at baseline (0 h) was as expected close to 100% (99.60 ± 0.08%), and decreased faintly, but significantly ($p<0.01$), after 24 h of incubation under normal gravity (95.39 ± 0.47%) and s-µG (95.96 ± 1.32%). No significant difference in T cell viability was observed between the *1 x g* or s-µG groups. Statistical confirmation was reached using one-way ANOVA with Bonferroni's multiple comparison post-hoc tests. This data indicates that there is a minor time-dependent decrease in T cell viability, which is unaffected by the gravitational condition. Taken together, this data suggests that the applied experimental approach does not induce a disproportional amount of cell death associated with either *1 x g* or µG-simulation in closed cryotubes. Nonetheless, this data does not give information about T cell functionality, such as antigen-dependent immune activation, proliferation, cytokine production or other effector functions.

Studying cytokine profiles under simulated spaceflight conditions

The second objective of my thesis focused on evaluating the CMI response resulting from different immunogenic challenges during *in vitro* simulation of µG and/or spaceflight-induced psychological stress. Changes in the CMI response were assessed using the *in vitro* DTH assay followed by downstream applications such as Luminex to quantify the evoked cytokine responses.

Evaluation of the immune cell-mediated immune response using the in vitro DTH assay

The *in vivo* DTH skin test (i.e. multitest CMI; Mérieux, Lyon, France) was a well-established and validated measure to monitor the CMI in humans. The mechanism of this test was based on the intracutaneous administration of antigens in the forearm, thereby evoking a measurable skin reaction that reflects the efficiency of the overall antigen-mediated immune response (42). However, due to increased risk of antigen sensitization when applied repeatedly on the same individual, the *in vivo* skin test phased out in 2002.

Alternatively, Feuerecker and his colleagues developed an *in vitro* DTH assay, capable of monitoring recall antigen-induced memory T cell reactions (33). Accordingly, this implies that a subject could only initiate a cell-mediated immune response, if he/she had residual memory lymphocytes that originated from a previous encounter of the same type of antigenic stimulus. In this project, bacterial antigens from the Boostrix vaccine (i.e. combined diphtheria-, tetanus- and pertussis-toxoid vaccine) were selected in order to induce the *in vitro* DTH response. This selection was based on the well-established (re-)vaccination program of the Boostrix vaccine within the Belgian community. Therefore, the immune system of most subjects should have retained specific memory T cells that can trigger a memory immune response after re-exposure to the recall antigens. In addition to antigen-dependent physiological immune cell activation (i.e. recall antigens), "artificial" lymphocyte activators were used as well to assess the CMI response evoked through different immune cell activation mechanisms. Firstly, monoclonal mouse antibodies against human CD3 and CD28 were used to trigger T lymphocyte mitosis through TCR-clustering (CD3), and co-stimulation (CD28) (16). Secondly, the plant lectin PWM was used to non-specifically induce T and B cell activation and proliferation in a monocyte-dependent way (35).

The impact of simulated microgravity on plasma cytokine levels.

Alterations in produced cytokine profiles were analyzed because of their competence to reflect global changes in the efficiency of the immune system. Plasma levels of IFN-γ, IL-2, IL-10 and TNF-α were measured after triggering of the immune reaction *in vitro* using different immunogenic challenges during µG-simulation. IFN-γ stimulates the activation of macrophages and has important immonuregulatory and antiviral properties (43). The secretion of IL-2 and binding to its receptor is a strong activation signal for the proliferation T cells (4). TNF-α has widespread pro-inflammatroy functions such as regulating cell proliferation and differentiation and is mainly secreted by macrophages (44). In contrast to IFN-γ, IL-2 and TNF-α, IL-10 has anti-inflammatory properties by downregulating the expression of pro-inflammatory (Th1) cytokines and early T cell activation genes such as NF-κB (45).

Analysis of the measured cytokine profiles (Luminex), showed a high variability in the intensity of the response between donors. Additionally, different cytokines displayed a varied response relating to the used challenge. This discrepancy could be explained by the intrinstic differences in activation mechanisms of the specific challenges. Nevertheless, clear indications were found that s-µG induced alterations in plasma cytokine concentrations. Physiological antigen-dependent stimulation of the immune cells with bacterial antigens induced notable increases in IFN-γ and IL-2 levels under normal gravity of *1 x g*. However, under s-µG those responses were inhibited, indicating that microgravity might impede pro-inflammatory cytokine production and subsequently the onset of CMI response. Gridley et al. also found decreased levels of IL-2 in space-flown mice and postulated that loss in IL-2 production could lead to an attenuattion of host's immune defenses against infections (20). In addition, gene expression studies have also shown that the IL-2R can be downregulated under s-µG, leading to impaired T cell activation (21).

Interestingly, the IL-2 response to monoclonal anti-CD3/CD28 antibodies was opposite compared to the response after stimulation with bacterial recall antigens (Boostrix). This inverse relationship could be caused by differences in the properties of the challenges. Accordingly, the response to recall antigens requires activation of memory T cells to elicit an antigen-dependent delayed immune response, whereas anti-CD3/CD28 antibodies act non-specifically on the complete T cell subset. Furthermore, the limited sample size and donor variability might also lead to a potentially skewed representation of the accurate effect among the population. In contrast to IFN-γ and IL-2, plasma levels of TNF-α and IL-10 peaked after stimulation with PWM for both *1 x g* and s-µG. Since IL-10 and TNF-α are both predominantly produced by, respectively monocytes and macrophages (i.e. instead of lymphocytes), it could potentially explain the differential cytokine response. Taken together, this data indicates that the cytokine response against immunogenic challenges can be altered under the influence of s-µG.

Immunomodulatory effects of stress hormones on plasma cytokine response under simulated microgravity.

During spaceflight astronauts are not only exposed to µG, but they are also prone to experience psychological stress. In this project we assessed whether supplementation of WB samples with stress hormones (HC) had an influence on the cytokine response profiles against different immunogenic challenges under s-µG. Many studies have reported the immunomodulatory role of stress hormones such as glucocorticoids (e.g. cortisol/hydrocortisone) and cathecholamines (e.g. adrenalin) (46). Moreover, it has been shown that stress hormones inhibit pro-inflammatory (Th1) cytokine production such as IL-12, IL-2, IFN-γ and TNF-α, but augment the production of anti-inflammatory (Th2) cytokines such as IL-10 and IL-4. Thus, the immune response is shifted from a Th1 into a Th2 cytokine response. This stress-induced immune inhibiting mechanism could, in part, be explained by a negative feedback pathway which protects the organism from generating an excessive, potentially tissue-damaging, pro-inflammatory cytokine response (47). However, the impact of stress hormones combined with µG-simulation is not yet understood completely.

In our experimental setup, we used varying concentrations of HC (i.e. 0-100-200-400-600 ng/ml) which reflect *in vivo* plasma cortisol levels of subjects experiencing differential states of mental stress. Supplementation with 0 ng/ml HC was used as reference control. Addition of 100-200 ng/ml HC mirrors the cortisol levels of unstressed individuals (48), whereas 400 ng/ml HC reflects a concentration comparable to highly stressed individuals. Finally, 600 ng/ml HC represented an unphysiologically high level of cortisol, seen in patients taking continuous glucocorticoid supplementation (33).

Plasma cytokine profiles were measured (Luminex) after peripheral blood was stimulated *in vitro* with immunogenic challenges and co-incubated with HC (i.e. 6 h pre-treatment plus additional 24 h with specific challenge). Results indicated that only the basal levels of the anti-inflammatory cytokine IL-10 (i.e. from unstimulated cells), displayed a rising trend under *1 x g* and s-µG in function of increasing HC concentrations. This finding is in line with the stress hormone-induced increase in Th2 cytokines (47). However, the IL-10 production after immune cell stimulation with different challenges did not result in measureable cytokine changes under s-µG.

In contrast, the concentration of pro-inflammatory cytokines TNF-α, IFN-γ, and IL-2 displayed a decreasing trend after stimulation with monoclonal anti-CD3/CD28 antibodies under s-μG. Additionally, TNF-α levels also showed a notable downward slope in function of increasing HC concentrations after stimulation with PWM. Taken together, observed changes in cytokine levels give an indication that stress hormones could have additional influence on the immune function. Nevertheless, more studies need to be performed in order to completely understand the interplay between mental stress and altered gravity conditions in space.

Future perspectives and general conclusion

With this study, more insight has been obtained in finding the underlying mechanisms of spaceflight-associated immune system weakening. However, the research needs to be continued by repeating ground-based spaceflight simulation experiments (i.e. expanding sample size) and through collecting in-flight data of ongoing and future space missions such as MoCISS. Comparing in-flight data with simulated spaceflight experiments on Earth is essential in order to validate the currently used spaceflight analogues as well as to assess the combined effect of all spaceflight stressors. Therefore, another important future goal is to implement IR in our experimental setup, because astronauts are inevitably subjected to both μG and IR in space.

Additionally, the collected cytokine data in this project can be supplemented with gene expression data of gravity-, ionizing radiation- and mental stress-affected genes. Currently the RNA extraction procedure is being optimized in order to proceed with identifying potential differentially expressed genes or pathways using microarray analysis. Accordingly, reverse transcription-PCR can be used to validate and quantify differentially expressed genes of interest. This genomic data is essential in order to identify the underlying molecular mechanisms causing the observed physiological changes related to spaceflight.

To conclude, the *in vitro* DTH assay is demontrated to be a valid tool for monitoring the global immune response in humans present on Earth or in space. Therefore, this assay was selected for MoCISS in order to evaluate the CMI of astronauts during a long-duration (6-month) spaceflight mission. Finally, this crucial in-flight data can be compared with data collected on Earth, thereby generating more insight in the harmful effects of spaceflight on the CMI.

V. Appendix

Supplemental figures

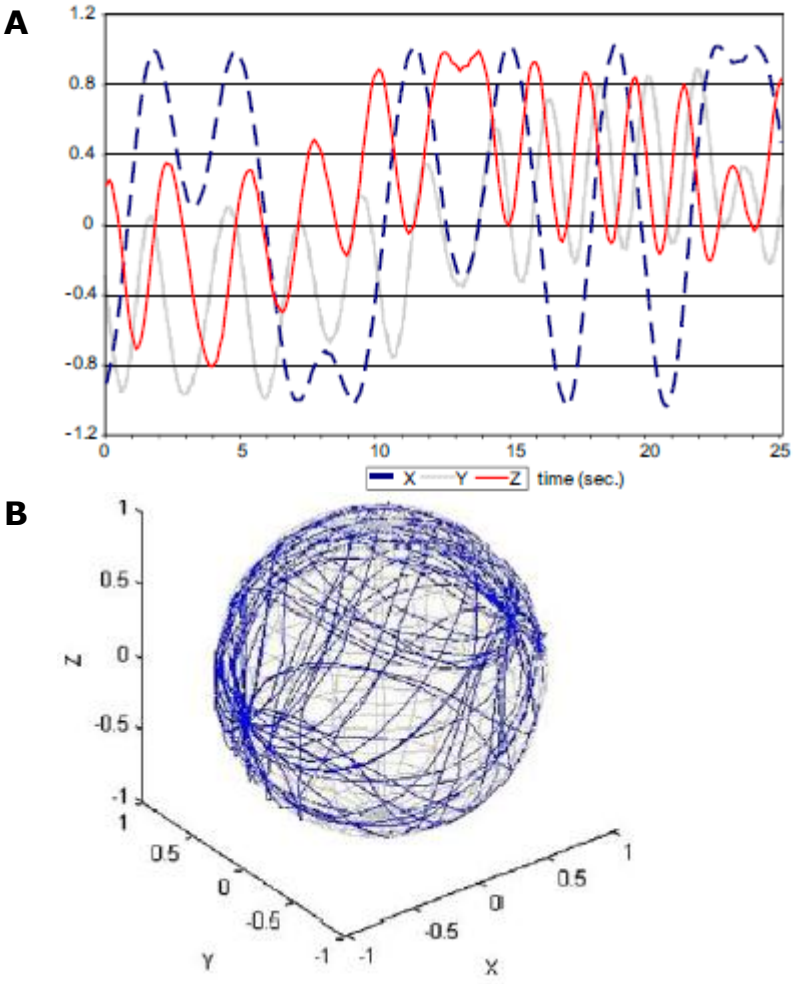

Supplemental figure 1. (A) Principle of the three-dimensional gravity vector averaging on the RPM, rotated in 3D random mode with random frame speed and direction. **(B)** Blue lines on the sphere visualize the motion trajectory in random speed and direction of a theoretical sample placed on the RPM. The abscissa in (A), as well as the X-, Y- and Z-axis in (B) refer to acceleration forces expressed in *g*. (Figure source: Borst et al. 2009)

Supplemental procedures

I. Detailed protocol of RBC lysis procedures

BD FACS 10 x Lysis Solution (BD Bioscience, Cat. No. 349202)

Aliquots of whole blood (100µl) or diluted blood (200µl; 50% v/v RPMI) were lysed for 10 min in 1.8 ml 1 x FACS lysing solution (10% v/v in MilliQ) in 2 ml Eppendorf tubes. After lysis, assay tubes were centrifuged for 5 min at 4400 rpm and supernatant was discarded. Subsequently, cells were washed once in 1 ml 1x PBS and centrifuged for 5 min at 4400 rpm. The cell pellet (isolated leukocytes) was used for further processing.

Cell Lysis Solution (Promega, Cat. No. A7933)

Aliquots of whole blood (100µl) or diluted blood (200µl; 50% v/v RPMI) were lysed for 10 min in 300 µl Cell Lysis Solution in 2 ml Eppendorf tubes. After lysis, tubes were centrifuged (5 min at 4400 rpm), supernatant was discarded and samples were lysed a second time with 300 µl Cell Lysis Solution. Supernatant was discarded as indicated before and cells were washed once in 1 ml 1x PBS and centrifuged for 5 min at 4400 rpm. The cell pellet (isolated leukocytes) was used for further processing.

II. Cytospin: leukocyte concentration onto glass coverslips for microscopic analysis

A Starfrost microscope glass (Waldemar Knittel, Germany) was placed inside the cytofunnel (Shandon EZ Double Cytofunnel, Thermo Scientific, USA) and two glass coverslips (round) were placed under the cytofunnel openings. Subsequently, the cytofunnel was closed without displacing the coverslips and 100 µl of sample was pipetted into the correct cytofunnel and centrifuged (Cytospin 4, Thermo Scientific, USA) at 900 rpm for 5 min. Afterwards, cytofunnels were opened and round coverslips, which now are coated with cells, were carefully removed. On top of the cell-coated sides one drop of mounting medium was added with or without DAPI (Vectashield, Vector Labratories). Excessive medium was removed and coverslips were fixed with nail polish. Finally, samples were analyzed microscopically.

III. Principles of Luminex technology

Luminex technology combines a bead-based sandwich Enzyme-linked Immunosorbent Assay (ELISA) with flow cytometry. The bead sets (i.e. magnetic microspheres) are internally dyed with different red-to-infrared fluorescent color tones. Moreover, each set is coated with monoclonal capture antibodies that are specifically targeted against one cytokine of interest. Simultaneous analysis of multiple cytokines is achieved through dual-laser flow cytometry, in which different bead sets and the reporter dye (i.e. streptavidin-Phycoerythrin) are analyzed by excitation with a red (635 nm) and green (532 nm) laser, respectively (Fig. A). Emission light from the excited reporter dye is proportional to the amount of bound markers on the beads.

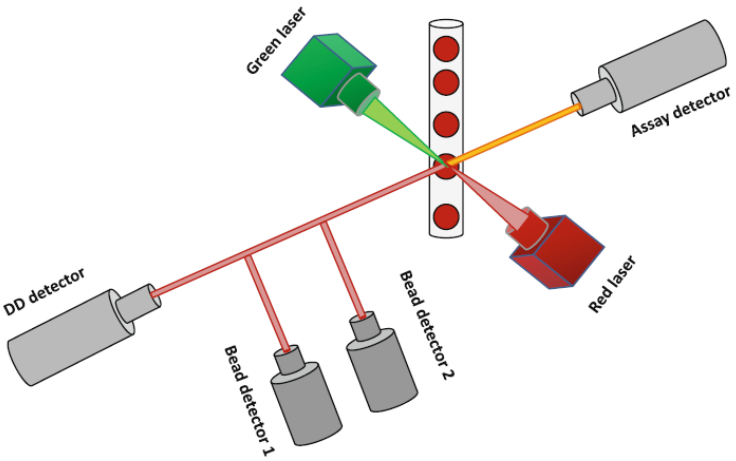

Figure A. Dual-laser flow-based bead detection. (Faresjo, M. 2014, Methods Mol Biol. 2014;1172:87-96)

References

1. Williams D, Kuipers A, Mukai C, Thirsk R. Acclimation during space flight: effects on human physiology. Cmaj. 2009;180(13):1317-23.
2. Yatagai F, Ishioka N. Are biological effects of space radiation really altered under the microgravity environment? Life Sciences in Space Research. 2014;3(0):76-89.
3. Clarke AH, Grigull J, Mueller R, Scherer H. The three-dimensional vestibulo-ocular reflex during prolonged microgravity. Exp Brain Res. 2000;134(3):322-34.
4. Gueguinou N, Huin-Schohn C, Bascove M, Bueb JL, Tschirhart E, Legrand-Frossi C, et al. Could spaceflight-associated immune system weakening preclude the expansion of human presence beyond Earth's orbit? J Leukoc Biol. 2009;86(5):1027-38.
5. Moreels M, de Saint-Georges L, Vanhavere F, Baatout S. Stress and Radiation Responsiveness. Stress Challenges and Immunity in Space. Berlin-Heidelberg, Germany: Springer-Verlag; 2012. p. 239-60.
6. United Nations Scientific Committee on the Effects of Atomic Radiation. UNSCEAR 2008 Report Vol. I Sources of ionizing radiation.
7. Zeitlin C, Hassler DM, Cucinotta FA, Ehresmann B, Wimmer-Schweingruber RF, Brinza DE, et al. Measurements of energetic particle radiation in transit to Mars on the Mars Science Laboratory. Science. 2013;340(6136):1080-4.
8. Hassler DM, Zeitlin C, Wimmer-Schweingruber RF, Ehresmann B, Rafkin S, Eigenbrode JL, et al. Mars' surface radiation environment measured with the Mars Science Laboratory's Curiosity rover. Science. 2014;343(6169):1244797.
9. Ainsbury EA, Bouffler SD, Dorr W, Graw J, Muirhead CR, Edwards AA, et al. Radiation cataractogenesis: a review of recent studies. Radiat Res. 2009;172(1):1-9.
10. Preston DL, Ron E, Tokuoka S, Funamoto S, Nishi N, Soda M, et al. Solid cancer incidence in atomic bomb survivors: 1958-1998. Radiat Res. 2007;168(1):1-64.
11. Morgan WF, Sowa MB. Non-targeted bystander effects induced by ionizing radiation. Mutat Res. 2007;616(1-2):159-64.
12. Johannes B, van Baarsen B. Stress Challenges and Immunity in Space. In: Choukèr A, editor. Psychological Monitoring. Berlin-Heidelberg, Germany: Springer-Verlag; 2012. p. 269-77.
13. Cohen S, Janicki-Deverts D, Miller GE. Psychological stress and disease. Jama. 2007;298(14):1685-7.
14. Kanas N. Expedition to Mars: Psychological, Interpersonal, and Psychiatric Issues. Journal of Cosmology. 2010;Vol 12:3741-7.
15. Kimzey SL. Hematology and immunology studies Johnson, R. S. Dietlein, L. F. eds. *Biomedical Results from Skylab* 1977,248-282 NASA Washington, DC, USA.
16. Crucian BE, Stowe RP, Pierson DL, Sams CF. Immune system dysregulation following short- vs long-duration spaceflight.: Aviation, Space, and Environmental Medicine,; 2008. p. 835-43.
17. Kaur I, Simons ER, Castro VA, Mark Ott C, Pierson DL. Changes in neutrophil functions in astronauts. 2004;18(5):443-50.
18. Kaur I, Simons ER, Castro VA, Ott CM, Pierson DL. Changes in monocyte functions of astronauts. Brain Behav Immun. 2005;19(6):547-54.
19. Rykova MP, Antropova EN, Larina IM, Morukov BV. Humoral and cellular immunity in cosmonauts after the ISS missions. Acta Astronautica. 2008;63(7–10):697-705.

20. Gridley DS, Slater JM, Luo-Owen X, Rizvi A, Chapes SK, Stodieck LS, et al. Spaceflight effects on T lymphocyte distribution, function and gene expression. J Appl Physiol (1985). 2009;106(1):194-202.
21. Boonyaratanakornkit JB, Cogoli A, Li CF, Schopper T, Pippia P, Galleri G, et al. Key gravity-sensitive signaling pathways drive T cell activation. Faseb j. 2005;19(14):2020-2.
22. Crucian BE, Zwart SR, Mehta S, Uchakin P, Quiriarte HD, Pierson D, et al. Plasma cytokine concentrations indicate that in vivo hormonal regulation of immunity is altered during long-duration spaceflight. J Interferon Cytokine Res. 2014;34(10):778-86.
23. Mermel LA. Infection prevention and control during prolonged human space travel. Clin Infect Dis. 2013;56(1):123-30.
24. Ilyin VK. Microbiological status of cosmonauts during orbital spaceflights on Salyut and Mir orbital stations. Acta Astronaut. 2005;56(9-12):839-50.
25. Stowe RP, Mehta SK, Ferrando AA, Feeback DL, Pierson DL. Immune responses and latent herpesvirus reactivation in spaceflight. Aviat Space Environ Med. 2001;72(10):884-91.
26. Pecaut MJ, Nelson GA, Gridley DS. Dose and dose rate effects of whole-body gamma-irradiation: I. Lymphocytes and lymphoid organs. In Vivo. 2001;15(3):195-208.
27. Gridley DS, Pecaut MJ, Dutta-Roy R, Nelson GA. Dose and dose rate effects of whole-body proton irradiation on leukocyte populations and lymphoid organs: part I. Immunol Lett. 2002;80(1):55-66.
28. Pecaut MJ, Dutta-Roy R, Smith AL, Jones TA, Nelson GA, Gridley DS. Acute effects of iron-particle radiation on immunity. Part I: Population distributions. Radiat Res. 2006;165(1):68-77.
29. Rizvi A, Pecaut MJ, Gridley DS. Low-dose gamma-rays and simulated solar particle event protons modify splenocyte gene and cytokine expression patterns. J Radiat Res. 2011;52(6):701-11.
30. McEwen BS. Protective and damaging effects of stress mediators: central role of the brain. Dialogues Clin Neurosci. 2006;8(4):367-81.
31. Yi B, Rykova M, Feuerecker M, Jager B, Ladinig C, Basner M, et al. 520-d Isolation and confinement simulating a flight to Mars reveals heightened immune responses and alterations of leukocyte phenotype. Brain Behav Immun. 2014;40:203-10.
32. Tingate TR, Lugg DJ, Muller HK, Stowe RP, Pierson DL. Antarctic isolation: immune and viral studies. Immunol Cell Biol. 1997;75(3):275-83.
33. Feuerecker M, Mayer W, Kaufmann I, Gruber M, Muckenthaler F, Yi B, et al. A corticoid-sensitive cytokine release assay for monitoring stress-mediated immune modulation. Clin Exp Immunol. 2013;172(2):290-9.
34. Borst AG, van Loon JWA. Technology and Developments for the Random Positioning Machine, RPM. Microgravity Science and Technology. 2009;21(4):287-92.
35. Crucian B, Sams C. Immune system dysregulation during spaceflight: clinical risk for exploration-class missions. J Leukoc Biol. 86. United States2009. p. 1017-8.
36. Vermes I, Haanen C, Steffens-Nakken H, Reutelingsperger C. A novel assay for apoptosis. Flow cytometric detection of phosphatidylserine expression on early apoptotic cells using fluorescein labelled Annexin V. J Immunol Methods. 184. Netherlands1995. p. 39-51.
37. Bossuyt X, Marti GE, Fleisher TA. Comparative analysis of whole blood lysis methods for flow cytometry. Cytometry. 30. United States1997. p. 124-33.
38. Tiirikainen MI. Evaluation of red blood cell lysing solutions for the detection of intracellular antigens by flow cytometry. Cytometry. 1995;20(4):341-8.

39. Boyum A. Isolation of mononuclear cells and granulocytes from human blood. Isolation of monuclear cells by one centrifugation, and of granulocytes by combining centrifugation and sedimentation at 1 g. Scand J Clin Lab Invest Suppl. 1968;97:77-89.
40. McFarland DC, Zhang C, Thomas HC, T LR. Confounding effects of platelets on flow cytometric analysis and cell-sorting experiments using blood-derived cells. Cytometry A. 2006;69(2):86-94.
41. Perfetto SP, Chattopadhyay PK, Lamoreaux L, Nguyen R, Ambrozak D, Koup RA, et al. Amine-reactive dyes for dead cell discrimination in fixed samples. Curr Protoc Cytom. 2010;Chapter 9:Unit 9 34.
42. Kniker WT, Anderson CT, McBryde JL, Roumiantzeff M, Lesourd B. Multitest CMI for standardized measurement of delayed cutaneous hypersensitivity and cell-mediated immunity. Normal values and proposed scoring system for healthy adults in the U.S.A. Ann Allergy. 1984;52(2):75-82.
43. Schroder K, Hertzog PJ, Ravasi T, Hume DA. Interferon-gamma: an overview of signals, mechanisms and functions. J Leukoc Biol. 2004;75(2):163-89.
44. Idriss HT, Naismith JH. TNF alpha and the TNF receptor superfamily: structure-function relationship(s). Microsc Res Tech. 2000;50(3):184-95.
45. Moore KW, de Waal Malefyt R, Coffman RL, O'Garra A. Interleukin-10 and the interleukin-10 receptor. Annu Rev Immunol. 2001;19:683-765.
46. Tian R, Hou G, Li D, Yuan TF. A possible change process of inflammatory cytokines in the prolonged chronic stress and its ultimate implications for health. ScientificWorldJournal. 2014;2014:780616.
47. Elenkov IJ, Chrousos GP. Stress hormones, proinflammatory and antiinflammatory cytokines, and autoimmunity. Ann N Y Acad Sci. 2002;966:290-303.
48. Jung C, Greco S, Nguyen HH, Ho JT, Lewis JG, Torpy DJ, et al. Plasma, salivary and urinary cortisol levels following physiological and stress doses of hydrocortisone in normal volunteers. BMC Endocr Disord. 2014;14:91.

Auteursrechtelijke overeenkomst

Ik/wij verlenen het wereldwijde auteursrecht voor de ingediende eindverhandeling:
Consequences of spaceflight stressors on cell-mediated immunity

Richting: **master in de biomedische wetenschappen-klinische moleculaire wetenschappen**
Jaar: **2015**

in alle mogelijke mediaformaten, - bestaande en in de toekomst te ontwikkelen - , aan de Universiteit Hasselt.

Niet tegenstaand deze toekenning van het auteursrecht aan de Universiteit Hasselt behoud ik als auteur het recht om de eindverhandeling, - in zijn geheel of gedeeltelijk -, vrij te reproduceren, (her)publiceren of distribueren zonder de toelating te moeten verkrijgen van de Universiteit Hasselt.

Ik bevestig dat de eindverhandeling mijn origineel werk is, en dat ik het recht heb om de rechten te verlenen die in deze overeenkomst worden beschreven. Ik verklaar tevens dat de eindverhandeling, naar mijn weten, het auteursrecht van anderen niet overtreedt.

Ik verklaar tevens dat ik voor het materiaal in de eindverhandeling dat beschermd wordt door het auteursrecht, de nodige toelatingen heb verkregen zodat ik deze ook aan de Universiteit Hasselt kan overdragen en dat dit duidelijk in de tekst en inhoud van de eindverhandeling werd genotificeerd.

Universiteit Hasselt zal mij als auteur(s) van de eindverhandeling identificeren en zal geen wijzigingen aanbrengen aan de eindverhandeling, uitgezonderd deze toegelaten door deze overeenkomst.

Voor akkoord,

Deckers, Sebastiaan

Datum: **9/06/2015**